A pilot study on the application of hydroacoustic surveys to assess the abundance of delaying sockeye in Georgia Strait:

A Final Project Report to the Southern Boundary Restoration and Enhancement Fund

by

Cory R. Lagasse, Yunbo Xie, Jacqueline L. Nelitz, Michael Bartel-Sawatzky

Pacific Salmon Commission,
600-1155 Robson St.
Vancouver, BC, Canada
V6E 1B5

October 2020

Correct citation for this publication:

Lagasse, C.R., Y. Xie, J.L. Nelitz, M. Bartel-Sawatzky. 2020. A pilot study on the application of hydroacoustic surveys to assess the abundance of delaying sockeye in Georgia Strait: A Final Project Report to the Southern Boundary Restoration and Enhancement Fund. Pacific Salmon Commission. October 2020.

TABLE OF CONTENTS

ABSTRACT

On dominant return years, Fraser River sockeye salmon (*Oncorhynchus nerka*) from the Late Shuswap stock group typically delay in the southern Strait of Georgia for a few weeks prior to river entry. This holding period provides fishing opportunities; however, assessing the abundance of milling sockeye is challenging in most years. Estimates have traditionally relied upon catch per unit effort (CPUE) data from PSC's Gulf troll test fishery. These estimates require very large expansion of CPUE (200,000 to 470,000) to determine total abundance, and this expansion factor can vary substantially within and across years, resulting in significant uncertainty around the estimates of abundance. In 2018, we conducted a mobile hydroacoustic survey in the southern Strait of Georgia to assess whether more accurate and precise in-season estimates of salmon abundance could be provided using hydroacoustic methods. From August 15 to September 12, weekly surveys were performed over an area of approximately 500 km^2 using a transecting vessel with a downward-looking split-beam echo sounder system. Acoustic data were analyzed using echo integration to estimate fish density and corresponding sockeye salmon abundance over the survey area. Biological information on species composition and fish length from Gulf troll catch samples informed the interpretation and estimation of acoustically detected fish schools. Hydroacoustic estimates of sockeye salmon abundance were compared to the in-season Gulf troll CPUE estimates and post-season reconstructed abundance estimates based on further seaward purse seine test fishery data and passage at the Mission hydroacoustics site in the lower Fraser River. The hydroacoustic estimate yielded a higher mean abundance of 3.9 million sockeye over the common survey period compared to the mean reconstructed abundance of 2.1 million and the mean Gulf troll estimate of 2.9 million. Hydroacoustics estimates were more variable among surveys compared to the reconstructed estimates, with a coefficient of variation of 43% vs 5% respectively, but less variable than the Gulf troll estimates where the coefficient of variation was 68%. Estimation of species composition and the mean target strength of sockeye are key areas of uncertainty that should be addressed to improve the accuracy of future surveys.

Key words: acoustic survey, salmon abundance, milling sockeye, sampling volume, fish density, echo-integration, volume backscattering coefficient, CPUE, Strait of Georgia, Fraser River

INTRODUCTION

Sockeye salmon (*Oncorhynchus nerka*) populations from the Fraser River, British Columbia, contribute to First Nations, recreational, and commercial fisheries that are important both economically and culturally. Commercial fisheries are managed by the Fraser River Panel (FRP), a management body within the Pacific Salmon Commission (PSC) composed of representatives from the United States and Canada which upholds legislation within the bilateral Pacific Salmon Treaty. Management decisions are informed by in-season monitoring programs that are aimed to estimate the daily abundances and total returns of Fraser River sockeye salmon.

In recent history, the abundance of Fraser River sockeye salmon returns has followed a cyclical pattern with a larger return occurring every 4 years. On these cycle years of large returns, the major population component is the Late Shuswap stock group, composed of populations from the lower Adams River and lower Shuswap River. These populations of sockeye typically mill within the Strait of Georgia (SoG) off the mouth of the Fraser River for 2-3 weeks as they prepare for entry into the river (Lapointe et al. 2003). This milling/holding period provides an important opportunity for commercial fisheries before the fish enter the river; however, assessing the abundance of these milling sockeye can be challenging. Estimates have traditionally relied upon catch per unit effort (CPUE) data from PSC's Gulf troll test fishing fleet. Gulf troll estimates use large expansion factors (in the order of 100s of thousands) to convert CPUE into abundance estimates. In addition, these expansion factors can vary substantially within and across years, which can result in significant uncertainty around the estimates of abundance.

Fisheries hydroacoustics monitoring is an alternative means of estimating salmon abundance that can be more accurate and precise than CPUE-based estimates when used appropriately in conjunction with catch data. For example, the Fraser River Panel relies on estimates of sockeye passage from the Mission hydroacoustics site in the lower Fraser River to verify and calibrate test fishing estimates from marine areas (Michielsens and Cave, 2019). The primary advantage of hydroacoustics is that it allows fish to be non-invasively observed throughout most of the water column, while test fishing methods can only obtain information on fish that are encountered with the deployed gear during limited sampling intervals and at limited locations. For salmon escapement assessment, fisheries sonars are typically used in a riverine environment to estimate the abundance of salmon migrating upstream. This technology has been implemented routinely in major salmon production rivers and lakes in North America to aid management of various fisheries and assessment of fish abundance (Mulligan 2000; Parker-Stetter et al. 2009). Hydroacoustic monitoring can also be applied to marine areas and is widely used by agencies around the world to estimate the abundance of pelagic and coastal fish populations (Simmonds and MacLennan, 2005).

Previous attempts have been undertaken to enumerate sockeye salmon abundance in the southern SoG using echo sounder technologies, though the most recent attempt was over 20 years ago. In 1986, the PSC carried out a series of surveys throughout the southern SoG using a dual-beam sonar (Levy et al. 1991), however, the predicted abundances of milling sockeye salmon were less than half the daily reconstructed estimates during the peak migration period. In 1998, Fisheries and Oceans Canada (DFO) attempted to assess sockeye using kilometer-long-range side-scan sonars,

but their surveys commenced too late in the season and by the time data collection occurred most sockeye salmon had already migrated into the river (Trevorrow and Farmer, 1998).

For this project, we conducted a series of weekly surveys during the period when commercial fisheries typically occur and milling sockeye abundance peaks in the SoG. Our surveys were undertaken in 2018, the dominant return year for Fraser sockeye and the only year on the four-year cycle when Late Shuswap sockeye and other populations consistently hold within the Strait prior to river entry (Lapointe et al. 2003; Hinch et al. 2012). Using a split-beam sonar towed by a vessel, we sought to assess whether a hydroacoustic method for monitoring could be a feasible alternative to marine test fisheries for in-season assessment of sockeye salmon abundance in the Strait of Georgia.

METHODS

Survey design

The study area for data collection was determined based on the expected distribution of delaying sockeye, logistical considerations, and the established survey design for the Gulf troll test fishery. Our original intent was to sample the entire width of the Strait of Georgia, from the eastern end of the southern Gulf Islands to the western end of Metro Vancouver's seashore; however, following the first weekly survey it was decided that such a design was inefficient and would, if completed within 2-3 days, result in a sparse distribution of transects that would not adequately sample areas near the mouth of the Fraser River where sockeye salmon were more likely to be concentrated. Therefore, our study area was restricted to an area of 493 km^2 covering the eastern half of the southern SoG (Figure 1). This study area closely overlaps with the sampling area of the PSC Gulf troll test fishery, as well as the main areas of commercial purse-seine and recreational troll fishing for sockeye within the SoG.

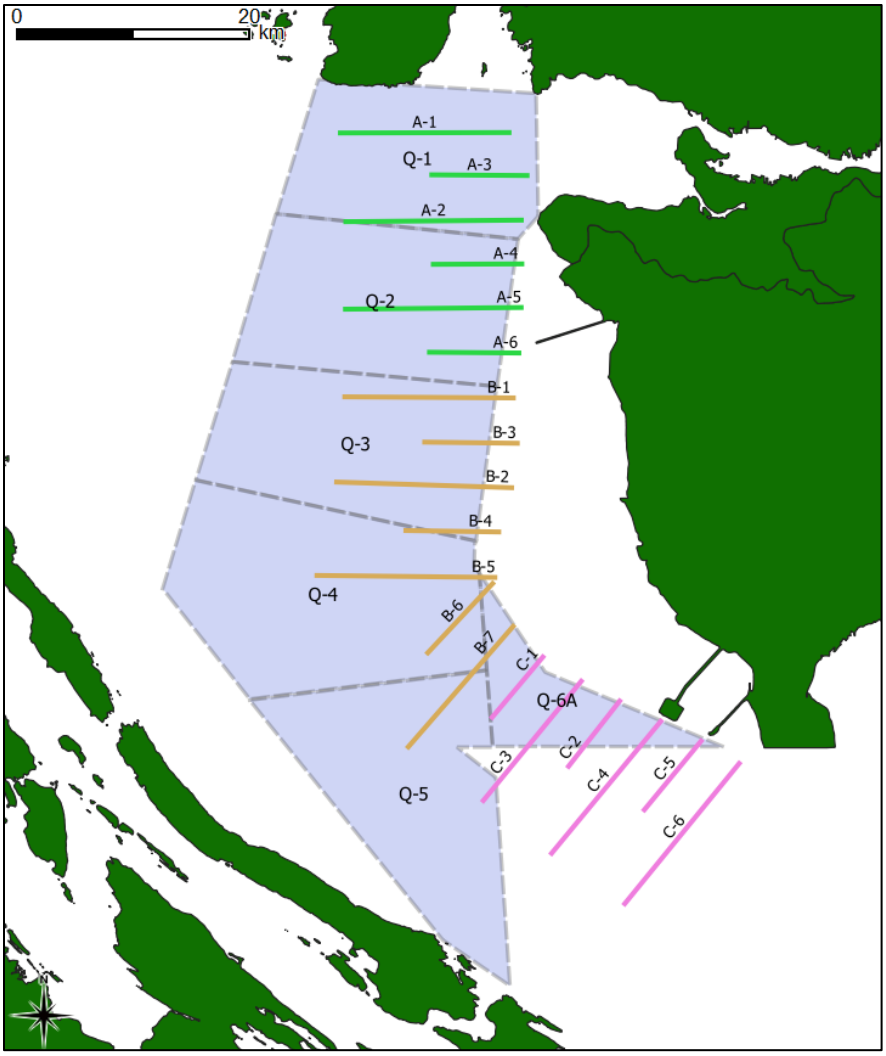

Figure 1. Survey quadrants (Q1-Q6A) for the PSC Gulf troll test fishery (blue polygons) with the hydroacoustic survey transect lines overlaid. Each colour of the transect lines represents a different planned day of data collection.

The bathymetry of the southern SoG consists of a sloping shelf with shallow tidal flats on the eastern end and depths increasing in the westward direction up to a maximum of 400 m. Based on prior surveys (Levy, Ransom and Burczynski, 1991) as well as empirical knowledge from test fisheries, we expected lower densities of sockeye salmon in deeper areas towards the middle of the Strait and higher densities in shallower waters closer to the mouth of the river. Therefore, to maximize survey precision, a stratified systematic design was adopted (Simmonds and MacLennan, 2005) with evenly spaced transects in a direction perpendicular to the shelf and a higher sampling effort within shallow areas compared to offshore deeper water areas as shown by the survey transect design in Figure 1. The start transect line for each survey was randomly chosen relative to the survey boundary area and spacing between transects. All transects were spaced approximately 2.5 km apart along their latitudes, with longer transects approximately 10 km in length alternating with shorter transects 5 km in length. Therefore, the offshore survey area was sampled half as intensively as the nearshore survey area. The offshore area was 256 km^2 and the nearshore area was 238 km^2. A total of 10 long transects and 9 short transects were planned for each survey, yielding 19 samples in the nearshore stratum and 10 samples in the offshore stratum.

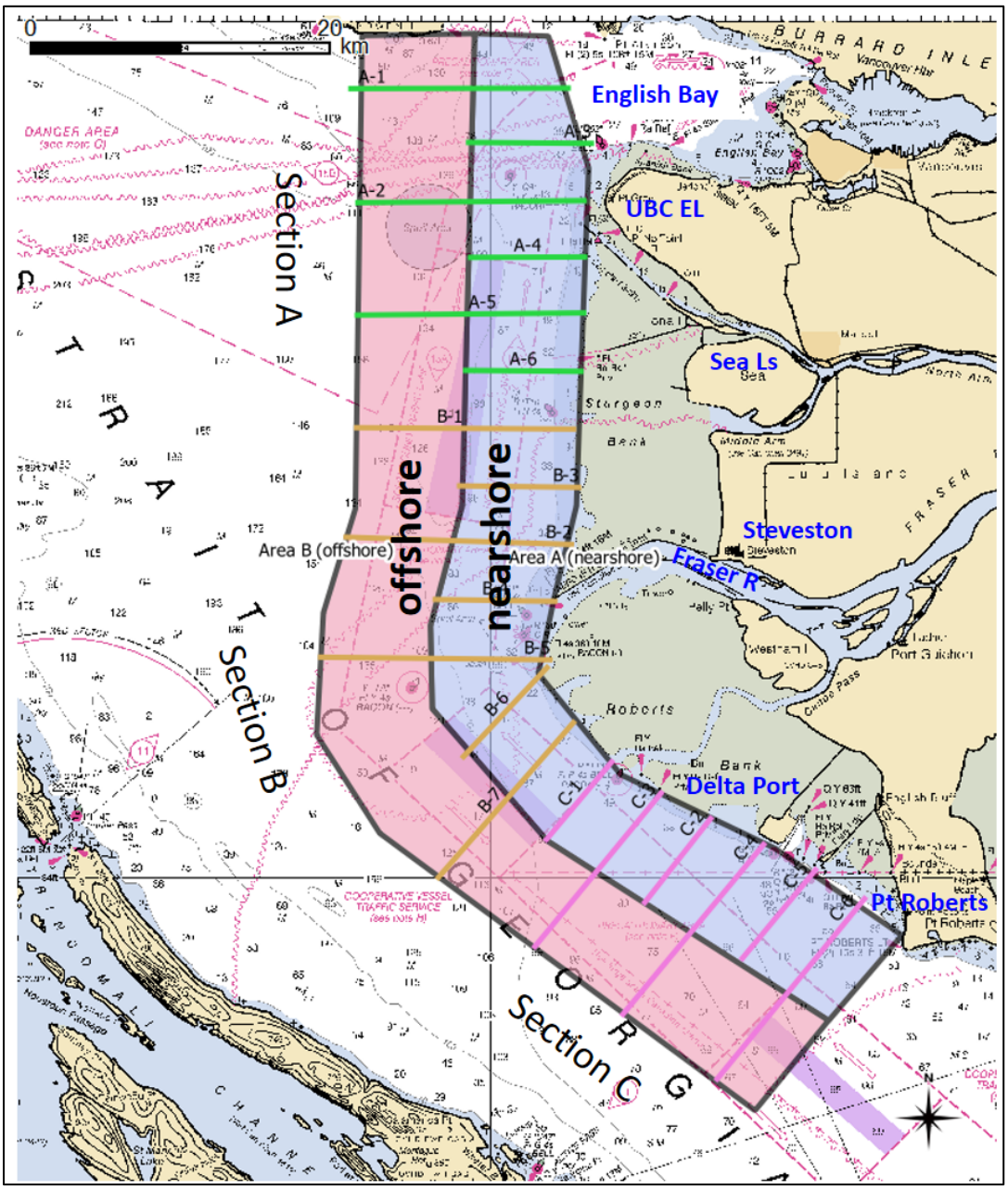

Figure 2. Study area including nearshore and offshore strata (blue and pink, respectively) and designated transect lines for surveys 2-5. The different colours for the transect lines each represent a sampling day. Six to seven transects were targeted for completion each day. The offshore stratum was sampled on every second transect to obtain half the sampling intensity compared to the nearshore strata.

Surveys were conducted between August 15 and September 12, 2018 during the period when Late Shuswap sockeye typically hold in the SoG. Five surveys of the study area were completed with each survey consisting of 2 or 3 days of transect data collection beginning on the Tuesday of each week. Transect dates and efforts are summarized in Table 1 for the 5 surveys. Survey 1 used a preliminary survey design sampling across the entire SoG with fewer transects, which was revised for subsequent surveys. Data was collected over a 10-12 hour period each day beginning at 6 a.m.

including travel time to the survey area from the Steveston Harbour. Surveys 3 and 5 included several short transects in the lower Fraser River, near the mouth of the river, where we expected sockeye to be found that were beginning their migration up the river. For surveys 4 and 5, the offshore portions of each transect were excluded due to time constraints imposed by rough weather. Based on low observed abundances of fish schools in the offshore area during the previous surveys, it was expected that this would not significantly affect the overall abundance estimates for these surveys. For survey 4, transects were not performed within the southern portion of the study area due to rough weather.

Table 1. Survey dates of data collection and number of transects completed and transect distance

Survey	Dates	# Transects	Transect Dist (km)
1*	Aug 15, 16	8	80
2	Aug 21, 23, 24	18	119
3	Aug 28, 29, 30	18	116
4	Sep 4, 6, 7	11	47
5	Sep 11, 12	17	70

*Survey 1 was based on a preliminary design with fewer transects covering a larger area.

Data collection

Hydroacoustic data was collected using a Biosonics DT-X split-beam echo sounder operating at a central frequency of 216 kHz with a 10.2° circular beam transducer. The transducer unit was housed inside a tow-body deployed from the starboard side of the survey vessel. The transducer was kept in a downward looking orientation and equipped with sensors to monitor its pitch, roll and bearing while being towed. A GPS unit was installed on the vessel to track the vessel's position and transect trajectories. The ping-by-ping echo data, the transducer orientation data and vessel's position data were all logged to a top-side PC using Visual Acquisition software (V6.3) with power supplies from the vessel's batteries converted to AC using a 2000W inverter. An 8.5 m long pleasure boat was used as the sampling platform for the first 4 surveys (Figure 3) and the final survey was conducted from an 8 m long commercial crabbing vessel. Vessel speed during data collection varied between 2.5-4 knots depending on sea swell and tidal flows with a mean transecting speed of 3.2 knots over surveys 2-5. Currents also acted on the tow-body during some transects causing variation in the roll and pitch of the transducer of up to ±15 degrees compared to a neutral position facing directly downward. Corrective actions were taken when the transducer's orientation was significantly deviating from the perpendicular by reducing the cruising speed and/or adjusting the heading of the vessel.

Figure 3. Grey Goose, the 8.5 m long pleasure cruiser used as a transect-sampling platform for surveys 1 to 4.

Data collection settings were adaptively adjusted during the surveys to improve data quality and to minimize acoustic noise impacts. During survey 1, a ping rate of 7.5 pings per second (pps) was used with a maximum sampling range of 70 m. Though most sockeye were expected to be present at water depths shallower than 60 m (Quinn, Terhart and Groot, 1989), the sampling range was increased to 100 m during survey 2 following reports from test fisheries that sockeye were swimming deeper than usual during the summer of 2018. The ping rate was correspondingly decreased to 5.5 pps to allow for the increased sampling range. For the final three surveys, sampling range was further increased to 130 m with a ping rate of 4.5 pps. When the bottom depth increased beyond 130 m, the ping rate was decreased to 2 pps and the sampling range increased to 250 m. The ping rate was decreased to eliminate bottom echoes from previous pings that may interfere with fish signals. The pulse duration was set to 0.4 milli-seconds for all data collection and the data collection threshold was set to -130 dB in terms of echo intensity level.

System calibrations of the DT-X system were performed in-situ within the study area during the surveys on August 9, 15, and 24. A Biosonics supplied tungsten carbide sphere of 36.4 mm in diameter was used as a standard target to verify the accuracy of target strength measurements produced by the DT-X. The sphere was suspended at a depth of approximately 10 m below the transducer using a fishing rod for positioning. The calibration data collected revealed that the average target strength readings were within an acceptable range of accuracy, with an average deviation less than ± 0.5 dB.

To determine and verify the speed of sound used for data collection and analysis, temperature-salinity-depth profiles were collected at the beginning location of each transect using an RBR Concerto CTD. Water property measurements were cast up to 80 m in depth at a sampling rate of

5 samples per second as the CTD was lowered through the water column. In all measurement locations, the sound speed based on measured temperature and salinity was between 1470-1510 m/s. For depths between 20 and 60 m where sockeye salmon were most likely to be found the sound speed ranged between 1480-1500 m/s. Variation in target strength measurements due to differences in the speed of sound was therefore assumed to be insignificant, and the default value of 1500 m/s based on surface temperature readings was used for acoustical ranging during all the surveys.

During hydroacoustic data collection, observations were also made for salmon jumping out of the water. The location and timing of any jumping salmon were recorded to enable matching these observations with hydroacoustic transect data.

Data processing

The data was processed and analyzed post-season to estimate sockeye salmon densities using echo integration (EI) methods (Foote, 1983; Medwin and Clay, 1998; Simmonds and MacLennan, 2005). Echoes collected by the DT-X sounder were stored as binary data files using DT4 Data File Format (Biosonics, 2008). The files were imported into Echoview software (V10.0, 2019) for visualization, editing and EI analysis. The principle of EI analysis is described in Appendix I. First, the GPS tracks of each transect were examined and any areas that deviated significantly from the intended bearing of the transect were excluded to avoid over or under representation of the intended sampling volume. A threshold was applied to the data to remove any signal (considered as noise) below a volume backscattering strength (SV) value of -70 dB (ref. $1m^{-1}$) for surveys 1 and 2. This threshold was subsequently increased to -65 dB for surveys 3, 4, and 5 to reject the increased volume backscattering noise level at greater sampling depths and ensure that fish schools could be adequately identified. The near-surface layer and bottom layer were excluded so that only acoustically valid sampling volumes were included in the analysis. The near-surface exclusion removed the first 2 m of sampling range and the bottom exclusion removed all data beyond the detected ocean bottom with an added offset of 0.5 m above the bottom to exclude any near-bottom noise or uncertain echoes from the acoustic blind zone off the bottom.

Once the data was verified and filtered, echo signals representing fish schools or individual fish targets were detected and isolated using the Echoview school detection module according to the methods of Barange (1994). Any echo clusters that exceeded a minimum size threshold and with SV above the threshold were identified as schools. The minimum size threshold was adjusted as required to ensure that no significant echo clusters were omitted. The detected schools were visually verified to remove echoes from plankton blooms, bottom reflections, turbulence, and other noise, leaving only schools that were inferred to represent fish.

Detected fish schools were classified into three categories: salmon schools, unknown schools, and forage fish schools. Criteria for classifications were determined in consultation with commercial trolling fishermen that have extensive experience interpreting fish signals on echograms (B. Van Dorp, pers. comms.), along with information on the location of jumping salmon recorded during the surveys, as well as expert judgement of experienced hydroacoustic technicians. The *salmon*

schools classification was assigned to schools that could most reliably be interpreted as sockeye salmon or other salmon species with the following distinctive features:

- schools were typically found at a depth between 20-70 m,
- had a higher echo strength reading (SV > -60 dB),
- were not closely associated with the sea floor,
- were more likely to be present in areas where salmon jumpers were observed, and
- occurred in well-defined patches that were not thinly dispersed amongst an area.

The species composition of salmon schools was assumed to be entirely sockeye salmon. The presence of other salmon species within the survey was likely minimal because no other major populations are present in the southern Strait of Georgia during August and early September on even years. This assumption was supported by catch in the Gulf troll test fishery for the survey period, which were composed of 99% sockeye salmon on average.

Estimates of sockeye abundance from integrated echoes of sockeye schools

The EI model links integrated echoes from fish schools to the volume density of the fish (see Appendix I for detailed descriptions of the method). According to the model, the relationship between volume backscattering coefficient sv (m^{-1}) and the volume fish density q_v (m^{-3}) for a single-species fish school is (see derivations of eq. (A23) in Appendix I):

(1) $$q_v = sv/\sigma_b$$

where σ_b (m^2) is the mean backscattering cross-section of individual fish in the school, whose estimation method is provided later. Since sockeye schools have a patchy distribution in the southern SoG, simply applying (1) to the entire designated survey area would have severely overestimated the total fish abundance in the basin. The analytical approach we developed for projecting the abundance in SoG consists of four steps:

1. estimate number of fish in individual schools;
2. estimate the total acoustical sampling volume within which these patchy individual schools are detected;
3. based on results from 1 and 2, calculate fish density for the entire sampling volume;
4. project total fish abundance for the designated survey area.

To accurately estimate fish abundance from acoustic samples, it is imperative that sampling volumes for individual schools and for an entire transect survey be accurately calculated. Foote (1991) proposed a modeling method to calculate effective acoustic sampling volumes by taking into consideration the shrinking effect of the 3-dB nominal beam-width as the signal-to-noise (S/N) ratio decreases with range as well as spatially non-uniform scattering of insonified targets. Models most relevant to sonar-beams transecting on sea or river/lakes surface to survey fish abundances were presented by Kieser and Mulligan (1984). Below, we follow Kieser and Mulligan (1984) to calculate sampling volumes for the SoG survey where effects due to low S/N ratio and non-uniform scattering of fish targets are ignored.

Acoustic sampling volume for individual fish schools

During hydroacoustic transects, fish schools are sampled by moving a downward-looking, cone-shaped beam projected by the transducer. Due to the patchiness of their spatial distribution, salmon schools are insonified by a truncated cone by a range bin within which a cluster of fish reside. If the acoustical ping rate is very low or the vessel is transecting the survey area at a very high rate of speed, the ping-to-ping sampling volumes do not overlap in space as shown in Figure 4.

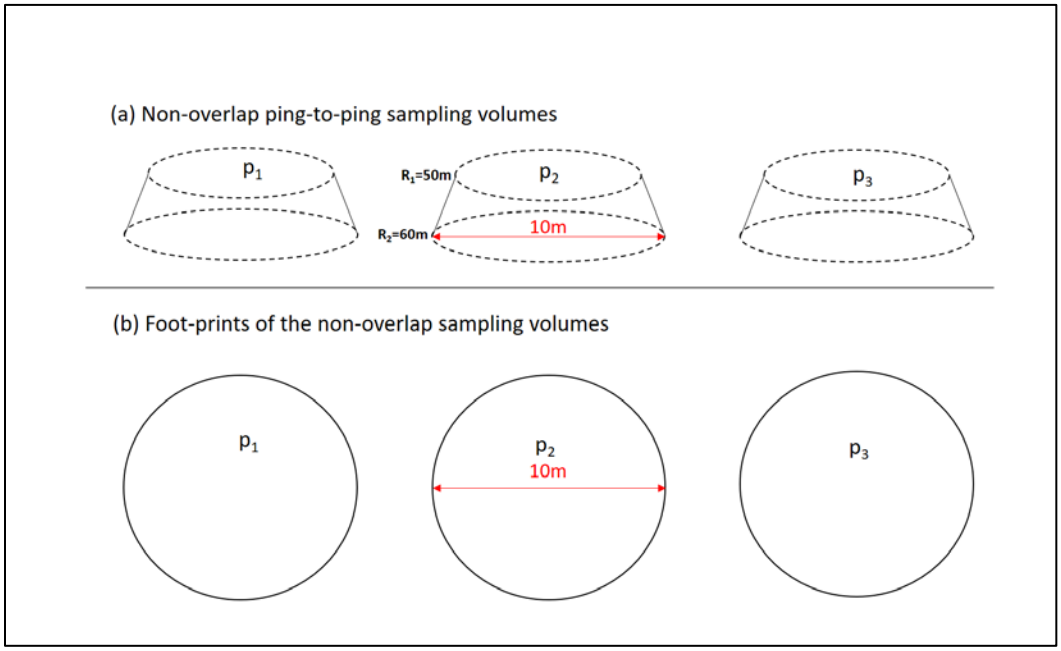

Figure 4. Schematic illustrations of 3 non-overlap ping-to-ping (p_1, p_2, p_3) sampling volumes projected by a 10-deg circular sound beam in a range bin of 55-60 m. (a) range-bin truncated cones; (b) foot-prints of the cones at a range of 60 m.

In our survey, most acoustic data were acquired at ping rates exceeding 4 pings per second from a vessel traveling an average speed of 3.2 knots or 1.6 m/sec. This setting produced a ping-to-ping vessel movement of less than 0.4 m per ping resulting in high overlapping of ping-to-ping sampling volumes as illustrated in Figure 5.

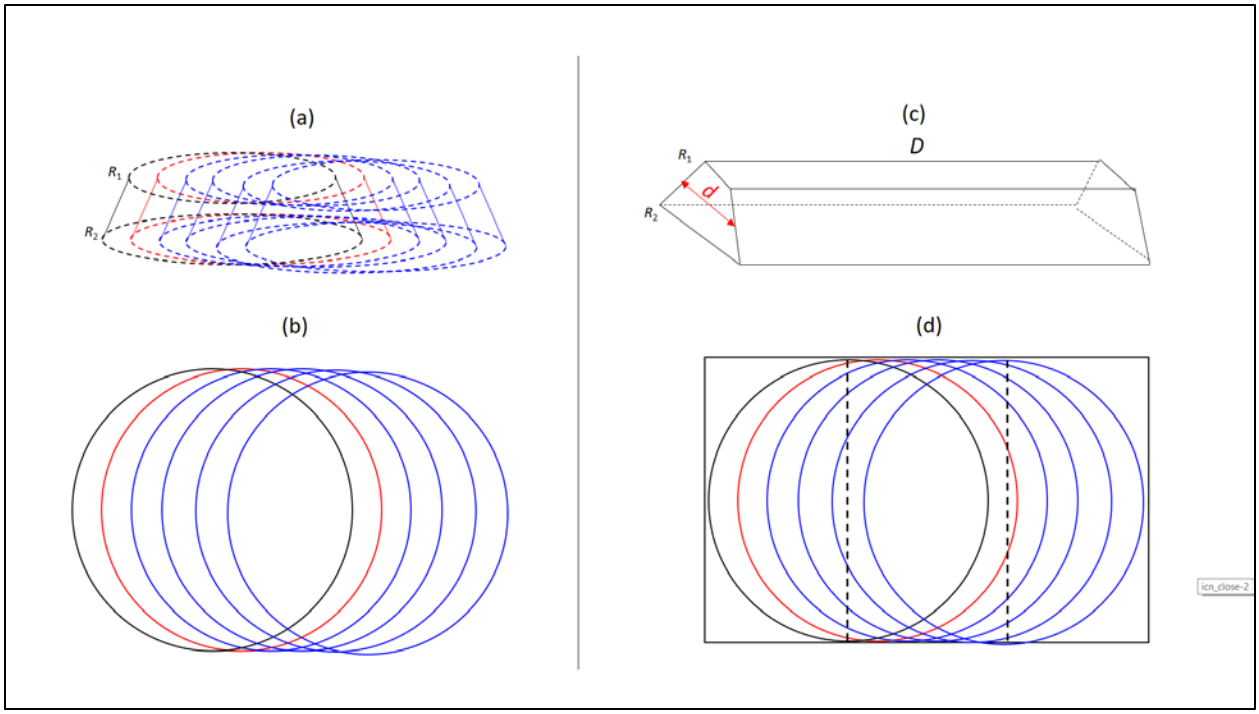

Figure 5. Illustrations of 6 highly overlapped ping-to-ping sampling volumes as the transducer's sampling volume slices through a school of fish at a range bin from R_1 to R_2. (a) 6 range truncated cones; (b) foot-prints of the 6 cones at R_2; (c) a trapezoidal prism to approximate the total sampling volume by the moving sampling cone where D is the transecting distance and d is the width of the prism at mid-range of $(R_1+R_2)/2$. (d) foot-print of the trapezoidal prism encompassing the foot prints of the moving cone where the two dashed lines demarcate the 2 edge volumes outside the dashed lines that need to be calculated for a truncated cone.

We adopted a modified trapezoidal prism model (Figure 5c) to calculate the sampling volume of detected fish schools by adding the edge volumes of the prism. The volume of the modified trapezoidal prism is:

(2) $$v = \Delta R \times d \times D + \Delta R \times \pi d^2/4$$

where d is the diameter of the cross-section of the truncated cone at mid-range of $(R_1+R_2)/2$, and $d = 0.5(R_1+R_2)\times\sin(bw)$ with bw being the full beam-width of the transducer in radians; $\Delta R = R_2 - R_1$ is the height of the cone; D is the transecting distance. The first term on the right-hand side (RHS) of eq. (2) is the volume of a trapezoidal prism, and the 2nd term is the volume of a cone sliced by a range-bin of ΔR.

Acoustic sampling volume of individual transects

The sampling volume geometry of an individual transect is represented by a wedge as shown in Figure 6.

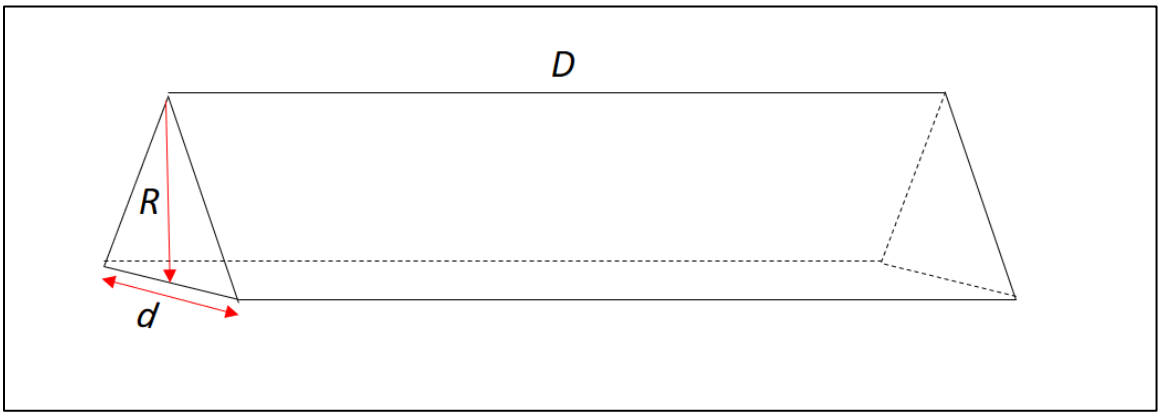

Figure 6. A wedge model for sampling volume of an individual transect. *R* is the maximum sounding range; *d* is the width of the wedge base; *D* is the transecting distance.

The sampling volume by the moving acoustic beam as shown in Figure 6 is

(3) $$V = \frac{1}{2}R \times d \times D + \frac{1}{3}R \times \pi d^2/4$$

where *R* is the maximum sounding range if the sounding range is less than sea-floor depth *H*; if the sounding range exceeds *H*, then *R* in (3) should be set to *H*; *d* is the width of the wedge base and is linearly increasing with *R* as $d = R \cdot \sin(bw)$. The first term on the RHS of eq. (3) is the volume of a wedge, and the second term is the volume of a cone with a height of *R* and a base diameter of *d*.

For the majority of survey transects, *R* was set to less than 200m and transecting distance *D* exceeded 1000m. With the 10-deg beam-width of the transducer, $d = R\sin(bw)$ is less than 35m. As a result, the edge volume represented by the 2nd term of (3) can be numerically ignored, and (3) takes an approximate form of

(4) $$V = \frac{1}{2}R \times d \times D = 0.5 \cdot R^2 \cdot \sin(bw) \cdot D$$

From (4) we can define a so-called effective sampling area *S* as

(5) $$S = V/R = 0.5 \cdot R \cdot \sin(bw) \cdot D$$

Note that *S* is constrained by *R*. Geometrically, the effective sampling area is the rectangle of the wedge's cross-section (Figure 6) at its mid-height of $\frac{1}{2}R$. Effective sampling area *S* is introduced for the convenience of extrapolation of observed fish density to other unsurveyed areas. However, it is important to note that *S* is linearly dependent upon range *R*. Since *R* can vary as the vessel

transects from deeper to shallower water, we use the mean range observed from individual transects to represent *R* when calculating *V* or *S*.

Estimation of total number of fish from a transect

For an identified fish school, we use (1) and (2) to calculate number of fish *n* in the school as

(6) $$n = q_v v = \frac{\overline{sv}}{\sigma_b} \cdot v$$

where $\overline{sv}$ is the mean volume backscattering coefficient over the number of acoustic pings probing the school.

If a total of M_j fish schools of single-species are detected from an individual transect *j*, we can calculate total number of fish N_j from this transect using (6) such that

(7) $$N_j = \sum_{i=1}^{M_j} n_i = \frac{1}{\sigma_b} \sum_{i=1}^{M_j} \overline{sv}_i \cdot v_i$$

where index *i* denotes variables associated with the *i*th fish school encountered in transect *j*.

The corresponding sampling volume and sampling area for transect *j*, as defined using (4) and (5), can be written as follows

(8) $$V_j = 0.5 \cdot R_j^2 \cdot \sin(bw) \cdot D_j \text{ , and}$$

(9) $$S_j = V_j / R_j = 0.5 \cdot R_j \cdot \sin(bw) \cdot D_j.$$

From (7)-(9), we can calculate fish densities for the local area surveyed by transect *j*. However, in this study, our objective is to estimate fish densities over the entire survey area.

Estimation of fish densities from all transects

Following Emmrich et al (2012), we consider the entire survey area as a single sample unit by pooling reflected energy from fish from all hydroacoustic transects. Suppose we conduct a total of *T* transects over the survey area, the overall fish densities in the area can be calculated as

(10) $$\rho_v = \sum_{j=1}^{T} N_j \,/\, \sum_{j=1}^{T} V_j$$

and the corresponding area density is

(11) $$\rho_s = \sum_{j=1}^{T} N_j \,/\, \sum_{j=1}^{T} S_j$$

This approach differs from that used by others such as Parker-Stetter et al (2009) who treated data from each transect as a single sample unit for fish density. The area-based density estimator (11) allows for assessment of variance of the sampling method rather than variance dominated by the spatial variation of fish abundance residing in different parts of the survey area. Using this estimator, fish abundances in the survey area are projected from observed densities from all transects within the area.

If the designated survey area comprises a total of K sub-areas of A_k (k = 1, 2, …, K), then fish abundance in A_k is projected as F_k and

$$F_k = A_k \times \rho_{s,k} = A_k \times \sum_{j=1}^{T} N_{j,k} \,/\, \sum_{j=1}^{T} S_{j,k} \tag{12}$$

Introducing index k (essentially a 2-dimensional variable) allows for an area stratification of fish abundance calculations within the area using (12). For instance, we can divide the survey area into two sub-areas with k=1 corresponding to the *nearshore* area and k=2 to the *offshore* area (see Figure 2). Using this stratification, variables on the RHS of (12) must be calculated for k=1 and 2, respectively, to obtain the projected abundances in nearshore and offshore areas. Finer stratifications of (12) can be readily implemented as well for northern, central and southern subareas within the survey area. In general, a 3-dimensional stratification of abundance calculations including the depth strata should be implemented by adding a vertical index h to (12) such that (12) takes a 3-d form of

$$F_{k,h} = A_k \times \rho_{s,k,h} = A_k \times \sum_{j=1}^{T} N_{j,k,h} \,/\, \sum_{j=1}^{T} S_{j,k,h} \tag{13}$$

where $\rho_{s,k,h}$ and $S_{j,k,h}$ are indexed with h meaning that both the fish density and the acoustic sampling area are depth-dependent. Due to limited transect sampling and schools of fish detected by the sonar system, especially in offshore area, in this report we only consider a single-depth stratum from the surface to sea-floor or to the maximum sounding range. We use formulae (12) to calculate abundances for designated *nearshore* and *offshore* areas by setting k to 1 and 2.

Estimation of variance of abundance projection

Multiple factors can cause estimation uncertainty due to random error in abundance projection as expressed by (12). These include relative orientations of fish to the sound-beam, non-uniform spatial distribution of fish within individual schools, effective sampling volume as a function of signal-to-noise ratio with increased range, as well as random acoustic measurement errors. In this report, we only assess variances due to non-uniform spatial distribution of fish within individual schools. For a given k (a subarea), (12) can be explicitly expressed by substituting (7) for N_j:

$$F_k = A_k \times \sum_{j=1}^{T} N_{j,k} \,/\, \sum_{j=1}^{T} S_{j,k} = A_k/\sigma_b \times \sum_{j=1}^{T} \left(\sum_{i=1}^{M_{j,k}} \overline{sv}_i \cdot v_i \right) / \sum_{j=1}^{T} S_{j,k} \tag{14}$$

We assume that all the variables except $\overline{sv}_i$ on the RHS of (14) are non-random, and the volume backscattering coefficients are uncorrelated among fish schools, i.e., $Covar(\overline{sv}_{i1}, \overline{sv}_{i2}) = 0$. Variance of F_k can then be expressed as

(15) $$Var(F_k) = (A_k/\sigma_b)^2 \times \sum_{j=1}^{T} \left(\sum_{i=1}^{M_{j,k}} Var(\overline{sv}_i) \cdot v_i^2 \right) / \left(\sum_{j=1}^{T} S_{j,k} \right)^2$$

If for fish school i, the sonar system projects a total number of P_i pings to acquire samples of the volume back scattering coefficient $sv_{i,p}$ (p=1, 2, …P_i) as the sound-beam moves across the school region, it follows that

(16) $$\overline{sv}_i = \left(\sum_{p=1}^{P_i} sv_{i,p} \right) / P_i$$

Assume that the ping-to-ping samples of $sv_{i,p}$ are independent and identically distributed (iid), the variance of $\overline{sv}_i$ is

(17) $$Var(\overline{sv}_i) = Var(sv_i)/P_i$$

where sv_i is the volume back scattering coefficient for fish school i. Substituting (17) into (15) leads to

(18) $$Var(F_k) = (A_k/\sigma_b)^2 \times \sum_{j=1}^{T} \left(\sum_{i=1}^{M_{j,k}} Var(sv_i) \cdot v_i^2/P_i \right) / \left(\sum_{j=1}^{T} S_{j,k} \right)^2$$

Thus, if the variance of sv_i is known or can be estimated, variance of F_k can be calculated from (18). A more intuitive form of (18) is to replace variable sv_i with density variable $\rho_i = sv_i/\sigma_b$, which leads to

(19) $$Var(F_k) = A_k^2 \times \sum_{j=1}^{T} \left(\sum_{i=1}^{M_{j,k}} Var(\rho_i) \cdot v_i^2/P_i \right) / \left(\sum_{j=1}^{T} S_{j,k} \right)^2$$

If coefficient of variation (CV_i) of ρ_i is available, (19) can be expressed in terms of CV_i and $\bar{\rho}_i$, the mean of ρ_i. Since

(20) $$CV_i = \sqrt{Var(\rho_i)}/\bar{\rho}_i$$

we have from (19) that

(21) $$Var(F_k) = A_k^2 \times \sum_{j=1}^{T} \left(\sum_{i=1}^{M_{j,k}} (CV_i \cdot \bar{\rho}_i \cdot v_i)^2/P_i \right) / \left(\sum_{j=1}^{T} S_{j,k} \right)^2$$

The advantage of (21) over (19) is that if ρ_i follows a heteroscedastic distribution, say, its standard deviation increases linearly with the mean, then the corresponding CV can be regarded as a constant. This will greatly simplify the calculation of $Var(F_k)$ by using (21).

Estimation of mean backscattering cross-section for sockeye

The mean backscattering cross-section σ_b is a measure of the acoustic size of interested fish species, in this case sockeye salmon. It is a key variable for determining fish abundance because it scales the signal strength of fish echoes to fish density or abundance; σ_b is related to *TS* via:

(22) $TS = log_{10}(\sigma_b)$ or $\sigma_b = 10^{0.1TS}$

In-situ measurements of sockeye *TS* were not conducted during our surveys due to time and resource constraints, therefore, measurements from the Mission hydroacoustics site, 70km upstream of the river mouth, were used as a substitute. The *TS* of fish were measured from a dorsal-aspect by a vessel transecting the river from September 15 to 19, 2018. During this period the vast majority of fish were Late Shuswap sockeye, as inferred from species and stock composition results from nearby test fisheries. A different Biosonics DT-X split-beam echo sounder was used for these measurements and operated at a central frequency of 210 kHz with a 6.3° circular beam transducer. *TS* measurements on the Biosonics system using a tungsten carbide sphere revealed a bias in default *TS* values, therefore an offset of 1.7 dB was applied to the median *TS* measurements to correct the measured values.

Gulf troll test fishery surveys

The Gulf troll test fishery has operated on years with abundant Late Run sockeye salmon since 1986. The area sampled by the surveys closely overlaps with the hydroacoustic survey areas (Figure 1), with trolling effort concentrated near the mouth of the Fraser River. Deeper regions further offshore are not sampled. The survey area is divided into six quadrants, with each quadrant receiving approximately eight hours of fishing effort for each weekly survey. In 2018, the test fishery consisted of two trolling vessels fishing within adjacent survey quadrants three consecutive days per week beginning on Tuesday. Test fishing surveys began on August 21 and occurred over similar time windows as hydroacoustic surveys 2 through 5. A weighted CPUE index for each test fishing survey was estimated by weighting each quadrant based on its proportional survey area.

To estimate sockeye abundance, a linear regression model is used to estimate the relationship between CPUE indices in the troll test fishery and milling sockeye abundance as determined retrospectively from run reconstructions. During the fisheries management season, the weighted CPUE indices from each survey period are used to predict the abundance of delaying sockeye based on the historical regression relationship. Different regression relationships are used to fit the data and determine abundance depending on the time of year and inferred behavior of salmon. In August, sockeye salmon are generally easier to catch and a regression relationship using only test fishing data from August is used to fit survey CPUE results from this period. In September, sockeye are less susceptible to fishing and survey CPUE results are fit to a regression relationship using only historical data from September. A regression relationship using only data from the dominant 4-year cycle is also considered as part of the sensitivity analysis on model predictions; however, this model was not adopted by the FRP in 2018 and is therefore not included in this report.

Post-season reconstruction to assess in-season delay estimates

To assess the accuracy of the hydroacoustic survey estimates, we compared them to the post-season reconstructed abundance of sockeye salmon. The reconstructed abundance likely represents the most accurate estimate of total milling sockeye salmon in the SoG and informs the official run size for Late Run sockeye salmon adopted by the FRP. The daily abundances of delaying salmon entering the SoG are calculated using a forward simulation of CPUE-based abundance estimates from seaward purse-seine test fisheries located in Juan de Fuca Strait and Johnstone Strait which was rescaled to total run sizes estimated from passage at the Mission hydroacoustics site plus seaward catch (Michielsens and Cave, 2019). The number of salmon exiting the SoG and entering the river on a given day is calculated from a backwards reconstruction of Mission estimates and lower river catches. It is assumed Late run sockeye need 4 days to travel from the marine test fishing locations to their milling area in the SoG. An additional 3-4 days of travel is required between the SoG and the Mission hydroacoustics monitoring site.

RESULTS

Estimated sockeye target strength, distribution and density

A total of 276 fish were measured for their TS from September 15-19 at the Mission hydroacoustics site, which resulted in a median TS of -35.5 dB. There were no apparent size changes as the fish entered the lower river from the SoG. The median nose-to-fork length of 1,277 sockeye caught from the Gulf troll test fishery was similar to that from the sockeye caught from the lower river test fishery (609 mm vs. 611 mm). After applying the offset of 1.7 dB measured from TS calibrations, a TS of -33.8 dB was obtained as representative of TS for the sockeye milling in the SoG, which leads to a sockeye backscattering cross-section σ_b of 0.00042 m^2.

Echo clusters on acquired echograms classified as salmon schools were detected in most transects for all five surveys (Figs. 7 and 8). General features of these salmon schools are summarized below:

1. Salmon schools were concentrated within the nearshore stratum at depths between 20 m and 70 m (Figure 9);
2. The five surveys identified a total of 812 schools of sockeye corresponding to 46,000 individual fish. Of the 812 schools, only 6 were located in offshore stratum (Figure 10) which accounted for 750 fish. Therefore, the offshore portion of the transects was only a minor contribution to the survey estimates of total sockeye abundance;
3. The spatial distribution of salmon schools changed with time over the five survey periods (see Figure 8). Salmon schools were small and sparsely distributed during Survey 1 (August 15-16), moderate abundances were observed primarily in the middle area in survey 2 (August 21-24), while for survey 3 (August 28-30) high densities of schools were observed in the southern section of the survey area. For survey 5 (September 11-12), highest abundances occurred off the mouth of the Fraser River.

4. Fish schools were not evenly distributed among transects in a survey, with some transects observing large schools while others observed no schools or only a few small schools (Figure 8).
5. Fish density increased steadily towards the end of August (Figure 11).

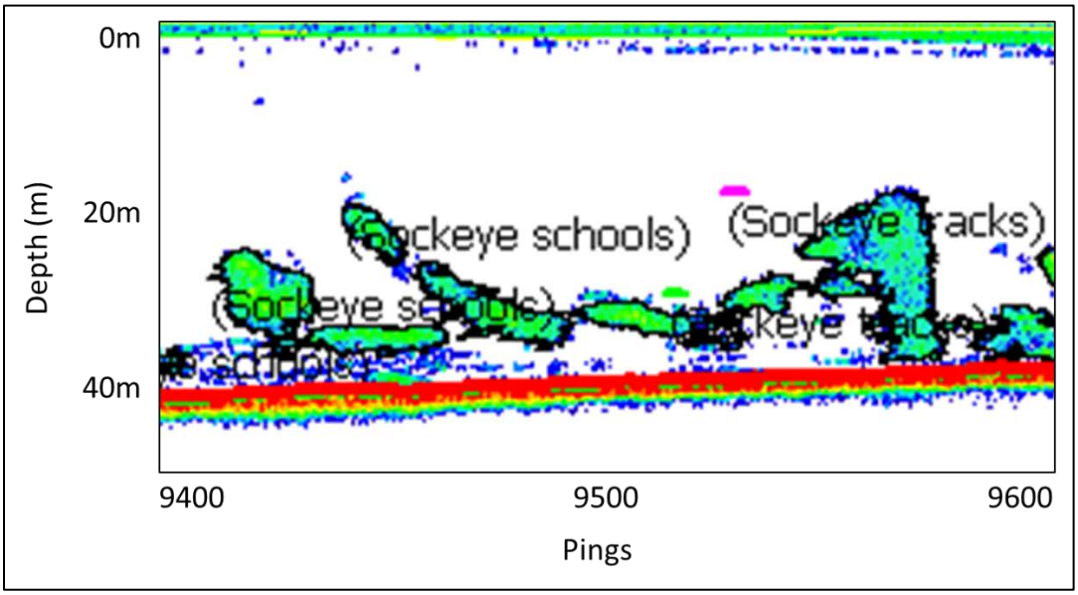

Figure 7. Echogram displays of fish schools identified and classified as sockeye schools shown as echo-clusters encircled with blacklines and labeled as “sockeye schools". Colours correspond to echo intensity level with red representing higher intensity and light blue lower intensity. The minimum volume backscattering level SV was set to -65 dB for the detection of sockeye schools. The data was collected on September 06, 2018 as the vessel was transecting from offshore towards Point Grey.

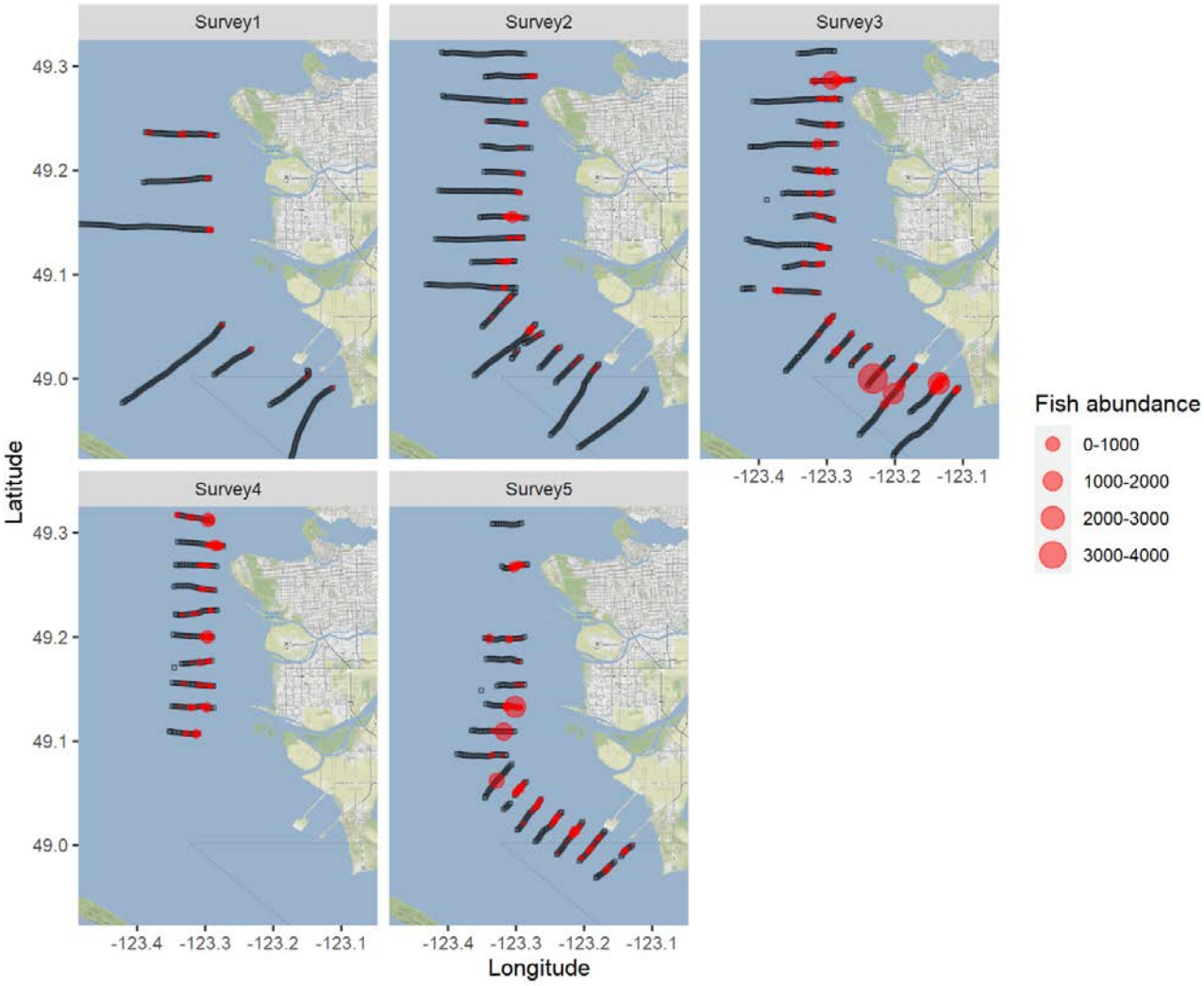

Figure 8. Cruise tracks of transects (black lines) and detected schools of fish (red circles) across the five surveys. All displayed latitudes and longitudes are in degrees.

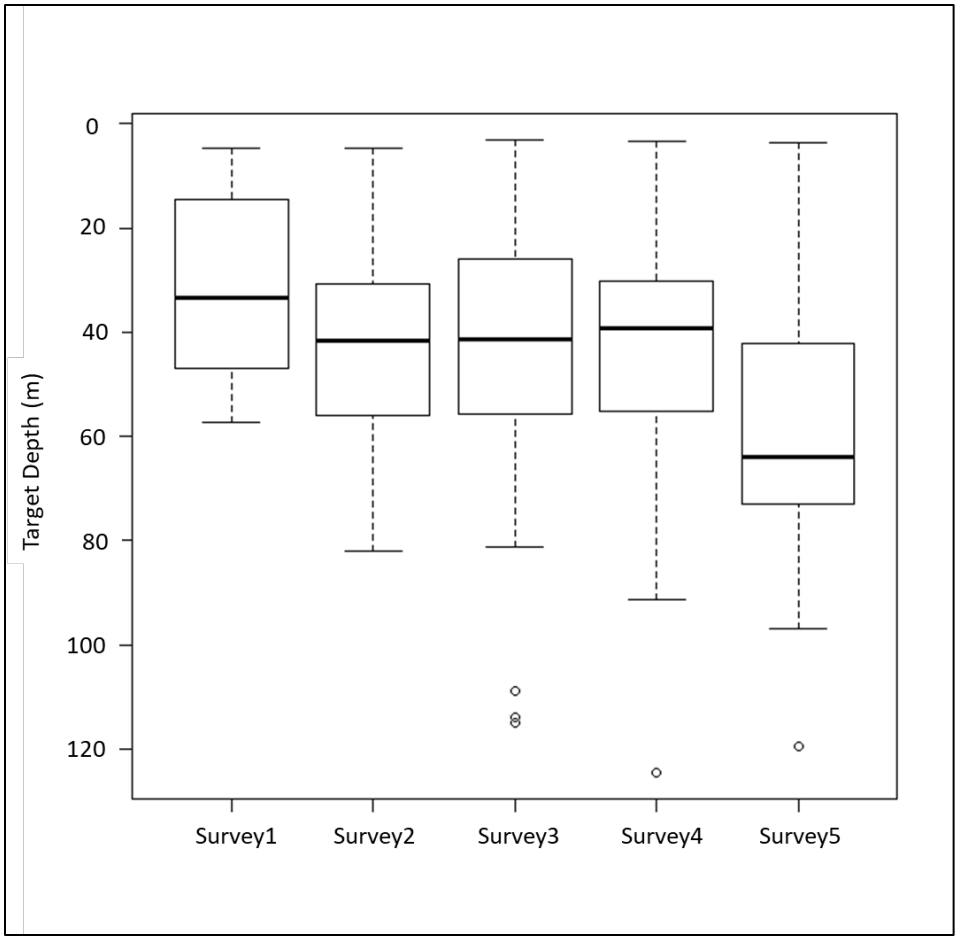

Figure 9. Depth distribution of salmon schools detected in each survey.

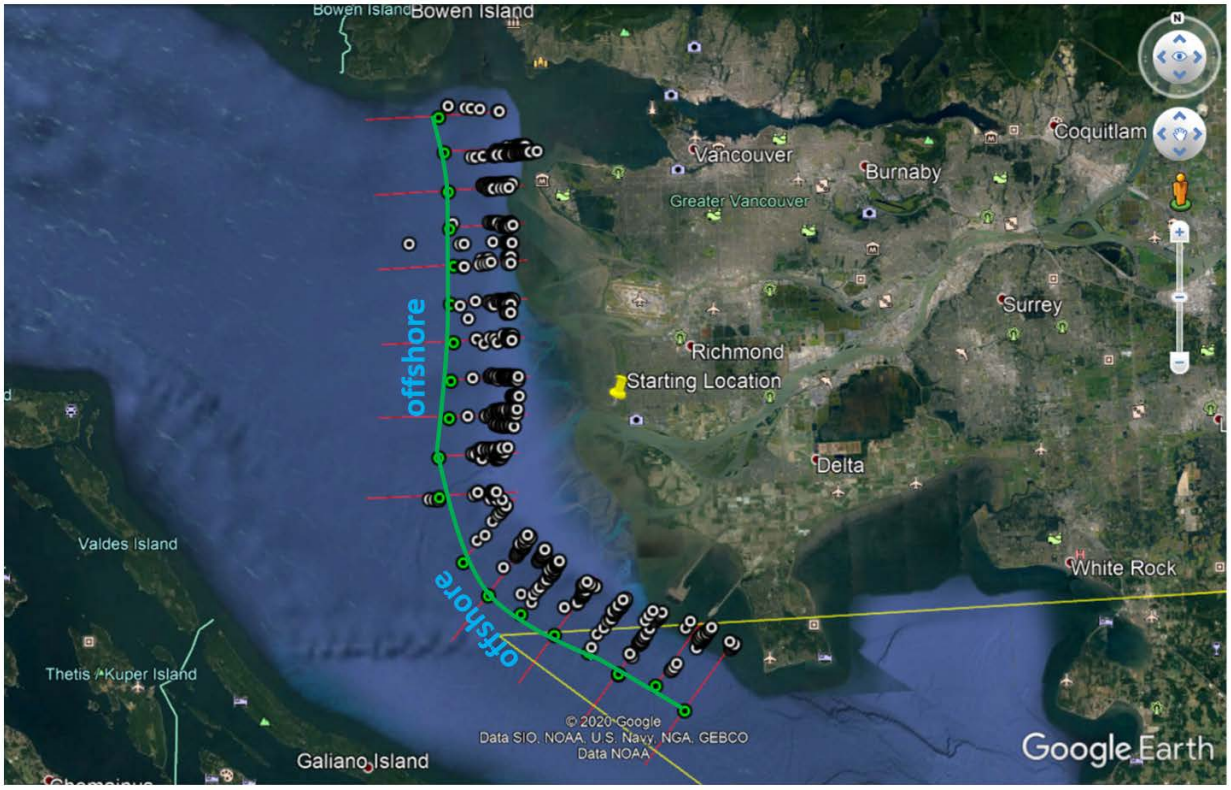

Figure 10. Distribution of salmon school locations (white circles) between nearshore and offshore strata. Green dots are demarcations on individual transect lines between the two strata; the green line is the border line separating the nearshore and offshore areas.

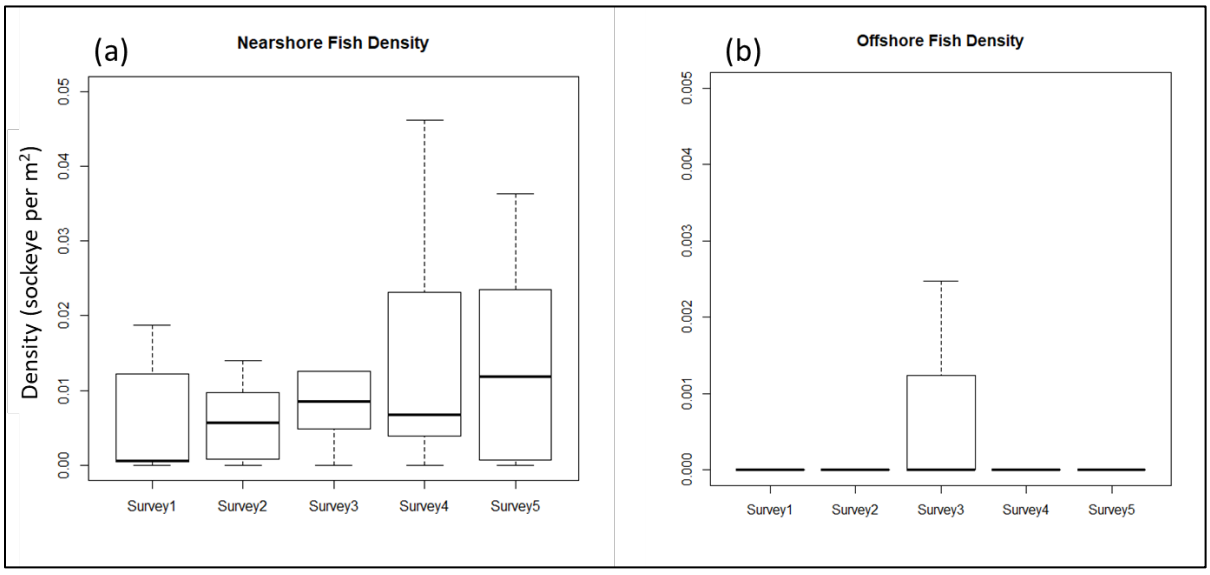

Figure 11. Boxplots of the distribution of average density of sockeye per unit area (m^2) observed in 5 transect surveys. (a) average densities for the nearshore stratum and (b) for the offshore stratum; most of the transects detected zero fish in offshore area.

Variance of the sockeye abundance estimate

The variance of the sockeye abundance is determined by variances of the acoustically estimated fish density of individual schools using equation (19) or (21). We did not estimate density variances for all 812 identified sockeye schools from Echoview. Instead, we semi-randomly selected fish schools at the lower quantile, median, and upper quantile of fish densities from each of the five surveys to perform the variance analysis. Using this selection criterion and software program FAST (Fisheries Acoustics Solution Tools) developed jointly by Vitech Research Consulting Corporation and PSC, we analyzed 15 density clusters of ping-by-ping samples for the five surveys. Figure 12 shows both the standard deviation of estimated fish density and coefficient of variation of estimated mean fish density for these 15 sockeye schools.

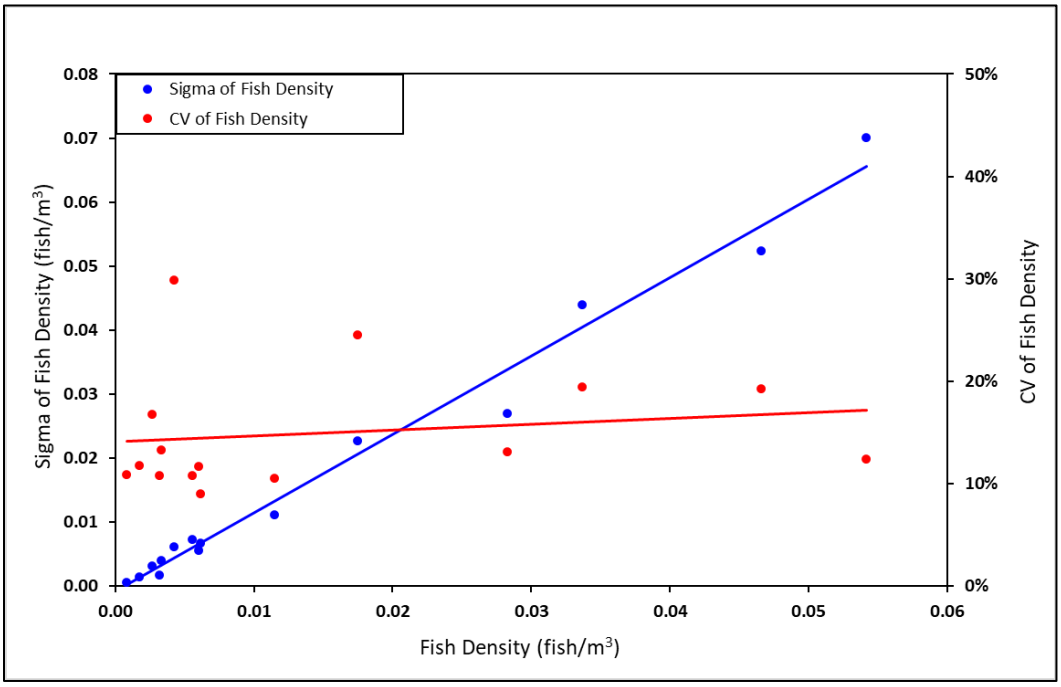

Figure 12. Standard deviation (*sigma*) of fish density and coefficient of variation (*CV*) of mean fish density estimated from the 15 acoustically detected sockeye schools from the five surveys. The two lines are the linear regression fits to the sigma (blue line) and *CV* data (red line) as functions of mean fish density.

From Figure 12, it is evident that the variance (or the standard deviation) of the measured fish density is proportional to the mean density. This implies that the measured fish density is a heteroscedastic random variable with a practically constant coefficient of variation of 15% over the observed range. Histogram analyses were performed on both the linear and logarithmical forms of the density data with quantile-to-quantile comparisons to a normal distribution. Analysis results are presented in Figure 13, which supports the hypothesis that the measured fish density is likely lognormally distributed. In the subsequent calculations of variance of abundance estimates, we use the coefficient of variation $\overline{cv}$ of 15% to represent variable CV in (21), which leads to

$$Var(F_k) = A_k^2 \times \overline{cv} \cdot \sum_{j=1}^{T} \left(\sum_{i=1}^{M_{j,k}} (\bar{\rho}_i \cdot v_i)^2 / P_i \right) / \left(\sum_{j=1}^{T} S_{j,k} \right)^2 \quad (23)$$

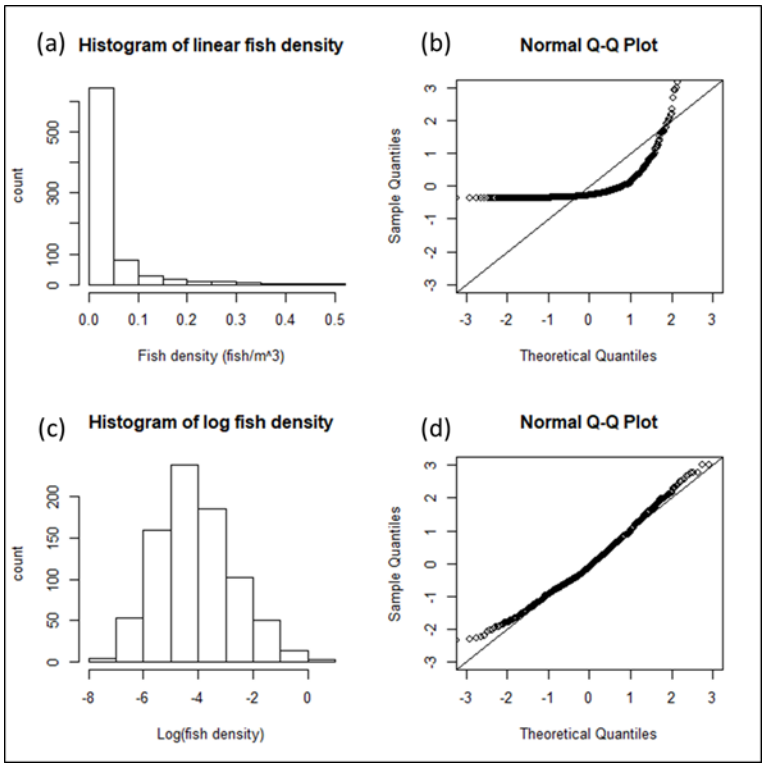

Figure 13. Histogram and quantile-to-quantile (w.r.t. normal distribution) analyses on the density data (a) and (b), and log form of the density data (c) and (d). The 1:1 lines provide a gauge on how close the data follows a normal distribution.

Weekly estimates of sockeye abundance based on the acoustic survey

Expanding mean fish densities across the survey area as shown in equations (12) and (23), we arrive at weekly estimates of sockeye abundance and their variances from the five surveys. Variances do not include error in the mean backscattering cross-section $\sigma_{b,}$ or species composition, which were assumed to be fixed for this study. Summaries of abundance estimates and corresponding coefficients of variation for each weekly survey are provided in Table 2.

Key features of the acoustic survey results are:

1. The weekly abundance reveals a temporal pattern from a lower abundance in mid-August to larger abundances towards the end of August and into September. This is consistent with the expected pattern for arrivals of Late run sockeye into the SoG, which typically hold there for 2-3 weeks before entering the Fraser River.
2. The majority of sockeye were found in the nearshore strata with a very small percentage of fish (<2%) found in the offshore strata.
3. The variance analysis by equation (23) produces a mean coefficient of variation of 5.1% for abundance estimates.

Table 2. Weekly sockeye abundance estimates and coefficients of variation (CV) by the hydroacoustic surveys in Strait of Georgia. Also shown are the key sampling effort data of individual surveys. The estimated areas are 238 km^2 for nearshore and 256 km^2 for offshore. Due to rough weather, survey 4 transects on September 6 & 7 could not be extended to the offshore area.

SURVEY	TRANSECT AREA (KM^2)		DETECTED NUMBER OF FISH		FISH DENSITY (FISH/KM^2)		ESTIMATED ABUNDANCE		CV OF ESTIMATED ABUNDANCE
	Nearshore	Offshore	Nearshore	Offshore	Nearshore	Offshore	Nearshore	Offshore	
1	0.21	0.26	607	112	5,066	734	1,205,821	187,928	6%
2	0.55	0.23	3,353	0	9,067	0	2,157,911	0	1.6%
3	0.79	0.53	21,154	639	24,911	697	5,928,792	178,537	5%
4	0.49	0.00	7,981	n/a	13,862	n/a	3,299,180	n/a	7.4%
5	0.64	0.07	12,079	0	16,392	0	3,901,229	0	5.8%

Comparison to Gulf troll and reconstructed abundances

Two fishing vessels participated in the Gulf troll test fishery in areas where the acoustic survey was concurrently conducted as shown in Figure 1. Catch data, CPUE, and species compositions are tabulated in Table 3 for approximately the same time period of the acoustic survey. Sockeye salmon represented 99% of the salmon caught and 97% of all fish caught over the four common survey periods. The Gulf troll expansion line (inverse of the sockeye catchability) was 200,000 using August data and 470,000 using September data, determined by the survey CPUE to the estimate of total sockeye abundance. The first Gulf troll survey from August 21 to 23 caught the highest number of sockeye. However, due to differences in the regression relationship and expansion lines that were used, the Gulf troll survey from September 4 to 6 resulted in the highest estimate of total sockeye abundance.

Weekly survey estimates of sockeye salmon abundance from the Gulf troll CPUE model were compared to corresponding hydroacoustic estimates for surveys 2 through 5 (Table 4). The Gulf troll CPUE estimate was similar to the acoustic estimate for survey 2 with an estimate of 2.1 million from the Gulf troll compared to 2.2 million from hydroacoustics. However, the hydroacoustic estimate of 6.1 million salmon more than tripled the Gulf troll estimate of 1.8 million for survey 3, while the opposite was true for survey 4 with the hydroacoustic estimate of 3.3 million salmon being significantly less than the Gulf troll estimate of 5.8 million. The hydroacoustic estimate of 3.9 million doubled the Gulf troll estimate of 1.9 million for survey 5. In general, the total sockeye salmon estimates produced by the two methods did not correspond, with major differences in the weekly survey estimates and the temporal trends in abundance (see Figure 14).

Table 3. Summary of species composition and sockeye CPUE for daily trips by the gulf troll test fishery in 2018. Each row represents a day of surveys for a single vessel. Two vessels fished concurrently within different quadrants of the survey area. Total fish catches include non-salmonid species such as spiny dogfish.

Trip Date	*Survey Quadrant*	*Sockeye Caught*	*Total Salmon Caught*	*Total Fish Caught*	*% salmon sockeye*	*% fish sockeye*	*Ave. CPUE Sockeye*	*Area weighted CPUE by Survey*
21-Aug-18	Q-1	18	18	18	100%	100%	0.71	
21-Aug-18	Q-2	319	320	320	100%	100%	12.78	
22-Aug-18	Q-3	140	143	162	98%	86%	8.06	Survey 2 CPUE: 12.2
22-Aug-18	Q-4	527	527	527	100%	100%	24.94	
23-Aug-18	Q-5	103	103	103	100%	100%	9.53	
23-Aug-18	Q-6	124	129	131	96%	95%	4.00	
28-Aug-18	Q-5	129	129	129	100%	100%	8.71	
28-Aug-18	Q-6	341	341	352	100%	97%	13.47	
29-Aug-18	Q-3	54	55	56	96%	96%	2.06	Survey 3 CPUE: 7.63
29-Aug-18	Q-4	201	201	202	100%	100%	7.99	
30-Aug-18	Q-1	182	183	199	99%	91%	7.42	
30-Aug-18	Q-2	307	308	309	99%	99%	9.64	
04-Sep-18	Q-5	108	109	110	98%	98%	8.73	
04-Sep-18	Q-6A	211	211	211	100%	100%	6.66	
05-Sep-18	Q-3	264	269	277	98%	95%	18.90	Survey 4 CPUE: 11.87
05-Sep-18	Q-4	490	490	492	100%	100%	18.77	
06-Sep-18	Q-1	77	77	81	95%	95%	2.64	
06-Sep-18	Q-2	197	197	201	99%	98%	7.27	
11-Sep-18	Q-5	14	16	20	70%	70%	0.71	
11-Sep-18	Q-6A	121	121	139	96%	87%	3.98	
12-Sep-18	Q-3	132	132	143	99%	92%	6.20	Survey 5 CPUE: 4.12
12-Sep-18	Q-4	277	278	295	100%	94%	9.71	
13-Sep-18	Q-1	3	3	4	75%	75%	0.15	
13-Sep-18	Q-2	15	17	18	88%	83%	0.46	

Table 4. Summary of delay sockeye estimates by the three methods based on surveys two to five. Also listed are the 80% probability intervals (PI) assuming abundance samples are normally distributed.

Method	**Survey2**	**Survey3**	**Survey4**	**Survey5**	**Mean**	**Sigma**	**80%PI**		***CV***
Hydroacoustics	2,157,911	6,107,329	3,299,180	3,901,229	3,866,412	1,659,684	1,739,441	5,993,383	43%
Gulf-Troll	2,117,000	1,750,000	5,821,000	1,889,000	2,894,250	1,957,023	386,223	5,402,277	68%
Reconstruction	2,068,889	2,309,253	2,143,748	2,075,968	2,149,464	111,742	2,006,261	2,292,668	5%

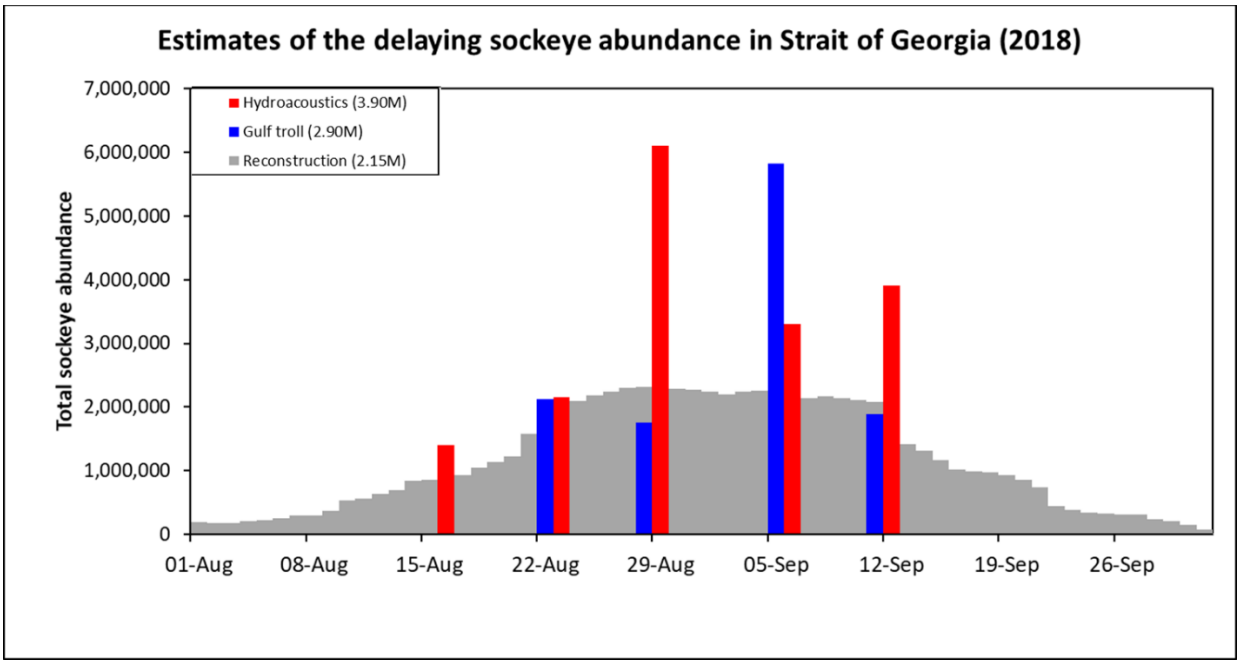

Figure 14. Delaying sockeye abundance estimates by the three methods. Estimated abundance by each method was the mean over the four weekly survey estimates from Aug 22 – Sept 12 (Survey 2-5).

The post-season reconstructed abundance of sockeye in the SoG increased throughout the month of August, reaching a maximum value of 2.3 million on August 28 as Late run sockeye salmon continued to migrate into the SoG and delay in the region prior to entering the Fraser River. Reconstructed estimates of sockeye abundance in the SoG remained fairly consistent from August 22 to September 11, with a minimum daily abundance of 2 million and a maximum of 2.3 million. Abundances declined from September 12 onward as the delay period ended and most Late run sockeye salmon began migrating up the Fraser River. On the contrary, weekly Gulf troll and hydroacoustic estimates were much more variable than reconstructed estimates during the delaying period from August 22 to September 12, with a minimum hydroacoustic estimate of total sockeye salmon of 2.1 million during survey 2 and a maximum estimate of 6.1 million during survey 3.

Treating the four weekly survey estimates by the three methods (Hydroacoustics, Gulf troll, and Reconstruction) as four samples of the same population, we arrived at three independent estimates of sockeye abundance quantified by the corresponding sample means. The Gulf troll estimated an average sockeye abundance of 2.9 million, hydroacoustic surveys estimated 3.9 million, and the reconstruction estimated 2.2 million. Therefore, the hydroacoustic survey produced the highest estimate of sockeye abundance in the SoG. Of the three methods, the reconstructed estimate has the lowest variance among surveys with a *CV* of 5% followed by hydroacoustic estimate with a *CV* of 43% while the Gulf troll estimate has the largest variance with a *CV* of 68%. The key summary statistics of the estimates by the three methods are listed in Table 4. The variances or uncertainties presented in Table 4 for individual estimates comprise both the temporal variability of the delaying sockeye abundance over the four weeks as well as measurement errors associated with the estimation methods.

DISCUSSION

This pilot study demonstrated the feasibility of using hydroacoustic surveys to estimate the abundance of milling/holding salmon in the SoG, providing a potential alternative to the Gulf troll test fishing surveys which are historically relied upon by the FRP to determine the in-season run size of Late-run sockeye salmon. A hydroacoustic survey design has now been developed that can be applied in subsequent years, and the EI analysis described in this report can readily be reproduced. With this methodology, in future years it should be possible to generate in-season estimates of the sockeye abundance delaying in the SoG using hydroacoustic surveys, assuming adequate resources and time can be allocated to data collection and analysis. The cost of conducting the pilot study was comparable to the charter cost for the Gulf troll test fishery.

Using a hydroacoustic method to estimate salmon abundance instead of test fishing can theoretically produce a higher precision estimate because of the larger area and higher number of fish sampled. In addition, hydroacoustic methods can be more readily standardized for consistency across years because there are no potential effects related to the experience and skill of the survey operator, as can occur with test fisheries. Furthermore, there should be no differences in hydroacoustic estimates due to changes in catchability within and across years as a result of fish behavior, if the fish remain distributed similarly within the survey area.

For the Gulf troll survey, changes in fish behavior and catchability are a significant source of uncertainty, and in most years the catchability shifts between August and September. In 2018, uncertainty in catchability for the Gulf troll model was significant, causing variability in the weekly survey estimates including a severe overestimate of abundance (5.8 million) from surveys on September 4 to 6. For other weeks in this study period, the Gulf troll did not overestimate abundance and produced an estimate that was similar to the post-season reconstruction.

The CV's of individual weekly hydroacoustic estimates range from 1.6% to 7.4% (see Table 2). Despite the high precision of the survey method, there were very large variabilities in the weekly estimates during this pilot study. Estimates of total salmon abundance peaked at 6.1 million during survey 3, then decreased to 3.3 million in survey 4 and then increased slightly to 3.9 million in the final survey. Comparisons to the reconstructed abundances suggest the hydroacoustic surveys produced a similar abundance estimate on August 22 (2.2 vs 2.1 million), overestimated on August 29 (6.1 vs. 2.3 million), and on September 5 (3.3 vs. 2.1 million), and on September 12 (3.9 vs. 2.1 million). The CV for our survey was determined based on variability in the acoustic measurements of fish density; however, errors from estimation of the mean acoustic back-scattering cross-section of sockeye, σ_b, and from species composition estimates were not included. These represent key areas of uncertainty for the hydroacoustic estimate and survey improvements to address this uncertainty are recommended in the section that follows. Uncertainty in the reconstructed estimate also bears consideration. Despite providing the best estimate upon which we can assess the hydroacoustic surveys, the reconstructed sockeye abundance is also subject to uncertainty, particularly during the arrival of sockeye into the SoG around August 22. The reconstructed abundance profile (shaded bar plot in Figure 14) shows apparently similar entry and exit durations. This needs to be confirmed from future surveys as the exit time of the delaying sockeye may be significantly shorter than the entry time because of their biological stimulus to migrate into the river.

A key question regarding the hydroacoustic survey is whether it can representatively sample the distribution of delaying sockeye within the SoG using a downward-looking sonar. Previous PSC surveys in 1986 (Levy et al. 1991) hypothesized that abundance was underestimated due to salmon staging in shallow waters that could not be accurately sampled. Trevorrow and Farmer (1998) investigated the use of a long-range side-scan sonar to enable the detection of sockeye in shallow waters on the flats of Roberts Bank; however, there were not enough salmon present to draw any conclusions. We were able to conduct our surveys in waters as shallow as a few metres depth, however, our effectiveness in detecting salmon was likely reduced due to boat avoidance behavior of fish, which has previously been observed using a similar survey platform in the lower Fraser River (Xie et al. 2008). Few fish schools were detected during our surveys at depths of less than 20 m, but the high estimates of total abundances throughout our surveys do not suggest that any major aggregations of salmon were not represented. If Fraser River pink salmon (*Oncorhynchus gorbuscha)* distribute themselves similarly to the sockeye salmon observed in this study, this survey design could be applied to estimate their in-season abundance as well; however, there are considerable knowledge gaps regarding the distribution and behaviour of pink salmon prior to their entry into the Fraser River.

Areas for further work

In order to reduce uncertainty and increase accuracy of the SoG hydroacoustic surveys, several areas for further improvement in the survey data collection and echo integration analysis should be investigated. In the following section, we identify some key areas for the improvement.

In-situ measurements of sockeye target strength

Density estimates of detected sockeye schools is sensitive to the mean acoustic backscattering cross-section σ_b. Since σ_b is related to sockeye target strength (*TS*) through a power relation of $\sigma_b = 10^{(0.1 \times TS)}$, accurate in-situ measurements of *TS* should be conducted to obtain representative dorsal-aspect *TS* data for sockeye salmon. The power relation between σ_b and *TS* leads to

$$\frac{d\sigma_b}{\sigma_b} = 0.23026 \times d(TS)$$

In terms of fish density q_v as defined in Equation (1), the above relative change in σ_b leads to a relative change in fish density estimate as

$$\frac{dq_v}{q_v} = -0.23026 \times d(TS)$$

Therefore, an error of one-decibel in *TS* estimate will result in a 23% relative error in density estimate. In this study, we have chosen -33.8 dB based on the *TS* measurements of these sockeye when they migrated past the lower river monitoring site at Mission. Had we chosen a *TS* value of -32.8 dB, we would have reduced the estimated sockeye abundance by 23%. The best practice is

to collect in-situ *TS* data for the fish in the SoG and use the median *TS* to derive fish density estimates from the EI data (Simmonds and MacLennan, 2005).

Employing a more seaworthy vessel for the survey

A larger, wider vessel would be more stable and better able to survey the SoG under high winds and swell. The chartered vessels were unable to survey when wind speeds exceeded 15 knots. As a result, survey 4 and 5 did not complete the intended number of transects, and survey 4 in particular was not able to representatively sample the entire survey area. During the survey period in August and September, high winds from the northwest are a common occurrence, so if the hydroacoustic surveys are to be relied upon for in-season estimation it will be important for the charter vessel to be able to survey in higher winds. Alternative tow body designs or specialized transducer deployments within the ship's hull would also improve data quality in adverse conditions by reducing transducer's pitch and roll movements.

Rigorous testing and calibration of echosounder *TS* accuracy

Estimates of fish abundance using EI analysis is critically sensitive to the measurement of *TS* by the transducer and echosounder because *TS* measurements are transformed into fish density. For our surveys, the Biosonics transducer and echo sounder were calibrated together in the winter prior to our surveys and in-situ *TS* measurements were collected following recommended protocols using a 36.4 mm (in diameter) tungsten-carbide (WC) sphere. These measurements confirmed the overall accuracy of the *TS* measurements, however, a decreasing trend of the *TS* reading with the increase target positioning in the Y-axis was observed and there were some concerns raised regarding the accuracy of the 10.2˚ transducer. These findings were reported back to Biosonics which attributed the inaccurate readings to using the 36.4 mm WC sphere and recommended a smaller WC sphere of 33.2 mm be used for the in-situ *TS* testing of this 216-kHz sounder system. For subsequent years it may be worth investigating alternative systems for the survey, including the Simrad EK60 which is more frequently used for collecting data for EI purposes.

Species verification and composition using mid-water trawls or purse seines

Hydroacoustic data cannot definitively identify the species within detected fish schools; therefore, mid-water trawls or purse seines are typically deployed to obtain catch samples from acoustically identified schools. This catch sampling should ideally be conducted throughout the survey period and area to capture changes in species composition over time and space. We verified species composition in this study using Gulf troll catch proportions, which were 97% sockeye salmon over the entire survey period. However, non-salmonid fish species have very limited susceptibility to troll fishing. The survey area is known to contain significant assemblages of Pacific herring (*Clupea pallasii*), particularly in the northern half. Using hydroacoustic data alone, we could not reliably distinguish herring or other species from salmon schools, and this may have been a source of overestimation of sockeye abundance in our surveys. For future surveys, purse seine sampling is recommended throughout the survey area to more accurately determine the proportion of sockeye salmon relative to all other fish species.

Establishing a baseline abundance of non-salmonid species

An alternative method for reducing uncertainty in species composition could be pursued by conducting hydroacoustic surveys before the arrival of milling sockeye and after they have exited the SoG. During these times, the abundance of salmon would likely be negligible, therefore, it could be assumed that all observed fish schools are non-salmonids and a non-salmonid abundance estimate could be derived. If we assume this baseline abundance does not change throughout the survey period, it could be subtracted from the total fish abundance during the delaying period to remove the influence of non-salmonid fish schools. Ideally this method would be tested in combination with purse seine fishing to reduce assumptions regarding stationarity of non-salmonid fish schools within the survey area.

Implementing a 3-dimensional model to obtain spatial structures of fish abundance

The analysis presented in this report used a large-scale 2-dimensional model to partition estimated fish abundance over a horizontal plane, i.e., on nearshore and offshore areas as explicitly expressed by (12). A finer model should include a vertical stratification as well for the abundance distribution as expressed by (13), i.e., a 3-dimensional model. The existing data could be reprocessed with a 3-d model, but the analysis was beyond the scope of the present study.

Implementing a geostatistical model for more precise total abundance estimates

The analysis in this report blended detected fish over the entire nearshore or offshore areas to estimate fish abundances over a very large area of >200 km^2 even though the spacing between adjacent transects from north to south was about 3 km. A geostatistical model can be applied to the transect data to improve the precision of the total abundance estimate and determine the spatial distribution of fish across the survey area.

ACKNOWLEDGEMENTS

We would like to thank Joe Enns for assistance in data collection and Li Ding for assistance with data processing, software development, and analysis. We would also like to thank Steven Stark and Tsawwassen Shuttles Incorporated for providing the charter vessel and logistical support for data collection. We are grateful to Eric Taylor and Merran Hague at the PSC for providing information on sockeye run reconstructions and the Gulf Troll test fisheries. This work was funded by the 2018-2019 Southern Boundary Restoration and Enhancement Fund of the Pacific Salmon Commission.

REFERENCES

Barange, M. 1994. Acoustic identification, classification and structure of biological patchiness on the edge of the Agulhas Bank and its relation to frontal features. South African Journal of Marine Science, 14: 333-347.

Echoview Software Pty Ltd (2019). Echoview software, version 10.0.288. Echoview Software Pty Ltd, Hobart, Australia.

Foote, K.G. 1983. Linearity of fisheries acoustics, with addition theorems. Journal of the Acoustical Society of America, 73(6):1932-1940.

Foote, K.G. 1991. Acoustical sampling volume. Journal of the Acoustical Society of America, 90(2):959-964.

Hinch, S.G., S. J. Cooke, A.P. Farrell, K.M. Miller, M. Lapointe and D.A. Patterson. 2012. Dead fish swimming: a review of research on the early migration and high premature mortality in adult Fraser River sockeye salmon *Oncorhynchus nerka*. Journal of Fish Biology, 81: 576 – 599.

Kieser, R., and T. J. Mulligan 1984. Analysis of echo counting data: A model. Can. J. Fish. Aquat. Sci. 41: 451-458.

Lapointe, M., S.J. Cooke, S.G. Hinch, A.P. Farrell, S. Jones, S. Macdonald, D. Patterson, M.C. Healey, G. Van Der Kraak. 2003. Late-run Sockeye Salmon in the Fraser River, British Columbia, are Experiencing Early Upstream Migration and Unusually High Rates of Mortality—What is Going On? Proceedings of the 2003 Georgia Basin/Puget Sound Research Conference.

Levy, D. B. Ransom and J. Burczynsky. 1991. Hydroacoustic estimation of sockeye abundance and distribution in the Strait of Georgia, 1986. Pacific Salmon Comm. Tech. Rep. no. 2: 45p.

Medwin, H., and Clay, C.S. 1998. Fundamentals of Acoustical Oceanography, Academic Press, Boston, 712 pp.

Michielsens, C.G.J., and J.D. Cave. 2019. In-season assessment and management of salmon stocks using a Bayesian time-density model. Can. J. Fish. Aquat. Sci. 76: 1073-1085.

Mulligan, T.J. 2000. Shallow water fisheries sonar: a personal view. Aquatic Living Resources, 13:269-273.

Parker-Stetter, S.L., Rudstam, L.G., Sullivan, P.J. and Warner, D.M. 2009. Standard operating procedures for fisheries acoustic surveys in the Great Lakes. Great Lakes Fish. Comm. Spec. Pub. 09-01.

Quinn, T.P., B. A. Terhart, and C. Groot. 1989. Migratory orientation and vertical movements of homing adult sockeye salmon, *Oncorhynchus nerka,* in coastal waters. Animal Behavior. **37**, 587-599.

Simmonds, J. and MacLennan, D. 2005. Fisheries Acoustics: Theory and Practice - 2nd ed. Blackwell Science Ltd.

Trevorrow M.V. and D.M. Farmer. 1998. Summary of Fisheries Sonar Field Evaluations in the southern Strait of Georgia, Sept. 1998. Acoustical Oceanography Institute of Ocean Sciences, Sidney, B.C. Canada.

Xie, Y., C. Michielsens, A.P. Gray, F.J. Martens, and J.L. Boffey. 2008. Observations of avoidance reactions of migrating salmon to a mobile survey vessel in a riverine environment. Can. J. Fish. Aquat. Sci. **65,** 2178-2190.

APPENDIX I: ECHO INTEGRATION MODEL

Echo Integration (EI) method originates from a single-fish backscattering physical model, which is expanded to a many-fish backscattering model.

Back scattering from a single fish

Backscattering by a single fish for a sonic wave in a non-absorptive, homogenous and isotropic medium is schematically outlined in Figure A1 on a spherical coordinate frame of radial distance R, polar angle θ, and azimuthal angle φ.

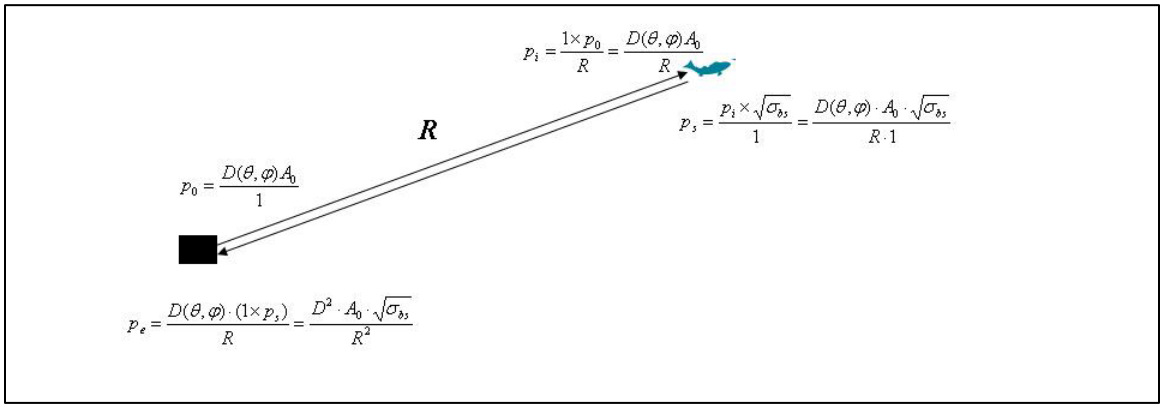

Figure A1. A scattering model from a single fish that links the transmitted sound by, and to received sound to, a monostatic sonar. Note: only the amplitudes of pressure signals are shown in the graph.

This model, as outlined by variables shown in Figure A1, links the transmitted sound $p_0(t)$ to received echo $p_e(t)$ from a single fish through three key physical processes detailed below.

Process 1: spreading of projected sound pressure: $p_0(t) => p_i(t)$

This is the most straightforward process of the three by assuming spherical spreading of the sound amplitude as $1/R$ over range. The pressure amplitude projected by a transducer at a reference range R_0 from the transducer is:

$$p_0 = \frac{D(\theta,\phi)\cdot A_0}{R_0} \qquad \text{(A1)}$$

where $D(\theta, \varphi)$ is the directivity of the transducer, and A_0, in *pascal·metre* as its dimension, is the source strength of the sound projected by the transducer. A_0 is uniquely determined by the amplitude of the volumetric deformation speed of the water by the pulsing piezoelectric ceramics of the transducer and the acoustic impedance of the water. Upon propagating over range R but just before impeding the fish, p_0 becomes p_i as an incident sound to be interacting with the fish:

$$p_i = \frac{R_0 \times p_0}{R} = \frac{D(\theta,\phi)\cdot A_0}{R} \qquad \text{(A2)}$$

where $R_0 \times p_0$ numerically represents the sound pressure projected by the transducer in the direction of (θ, φ) in a 3-d space. R_0 is conventionally chosen to be 1 m.

Process 2: scattering of the incident pressure by the fish: $p_i(t)$ => $p_s(t)$

This is the most complex process of the 3 as the fish can scatter the incident wave $p_i(t)$ with a complex scattering pattern. The complex scattering is simplified by introducing a 'scattering length' l which is the square root of the mean backscattering cross-section σ_{bs} defined as the product of the backscattering function of the fish and the intercepting area of the incident wave-front by the fish. Therefore, the incident wave is scattered by the fish with a scattering length of $l = (\sigma_{bs})^{1/2}$. The backscattering pressure at the 1-m range from the fish is:

$$p_s = \frac{p_i \times \sqrt{\sigma_{bs}}}{1}. \quad \text{(A3)}$$

Substituting (A2) into (A3) leads to

$$p_s = \frac{D(\theta,\phi)\cdot A_0 \cdot \sqrt{\sigma_{bs}}}{R \times 1}. \quad \text{(A4)}$$

Process 3: propogation of backscattering pressure p_s and its reception by the transducer as an echo from the fish: $p_s(t)$ => $p_e(t)$

This is a similar process to Process 1 except that the sound is emanated from the fish as a scattering sound of p_s, which propagates toward the transducer in the reciprocal direction to that of incident wave p_i. Since p_s must travel a distance of R in the direction of ($\theta + \pi$, $\varphi + \pi$) to arrive at the transducer, the received sound p_e by the transducer in the direction of ($\theta + \pi$, $\varphi + \pi$) is:

$$p_e = \frac{D(\theta+\pi,\phi+\pi)\cdot(1 \times p_s)}{R}, \quad \text{(A5)}$$

where $1 \times p_s$ numerically represents source strength of the sound pressure scattered by the fish. Substituting (A4) into (A5) and noticing that $D(\theta+\pi, \varphi+ \pi) = D(\theta, \varphi)$ by reciprocity, we can express p_e as an echo from the fish. This yields that

$$p_e = \frac{D^2(\theta,\phi)\cdot A_0 \cdot \sqrt{\sigma_{bs}}}{R^2}. \quad \text{(A6)}$$

Equation (A6) is the echo amplitude from a single fish for a single transmission of a sonic pulse (an acoustic ping) from the sonar. The complete waveform representation of the echo to a single-frequency continuous wave (CW) is:

$$p_e(t) = \frac{D^2(\theta,\phi)\cdot A_0 \cdot \sqrt{\sigma_{bs}}}{R^2} \cdot e^{-i2\pi f(t-2R/c)}, \quad \text{(A7)}$$

where f is the frequency of the CW wave and c is the sound speed of the water.

Backscattering from many fish

The single-fish backscattering model can be extended to backscattering from many fish. The many-fish scattering model is illustrated by Figure A2 with 3 individual fish confined within the space of a range shell ΔR, which is defined by the pulse-width of τ as $\Delta R = c\tau/2$.

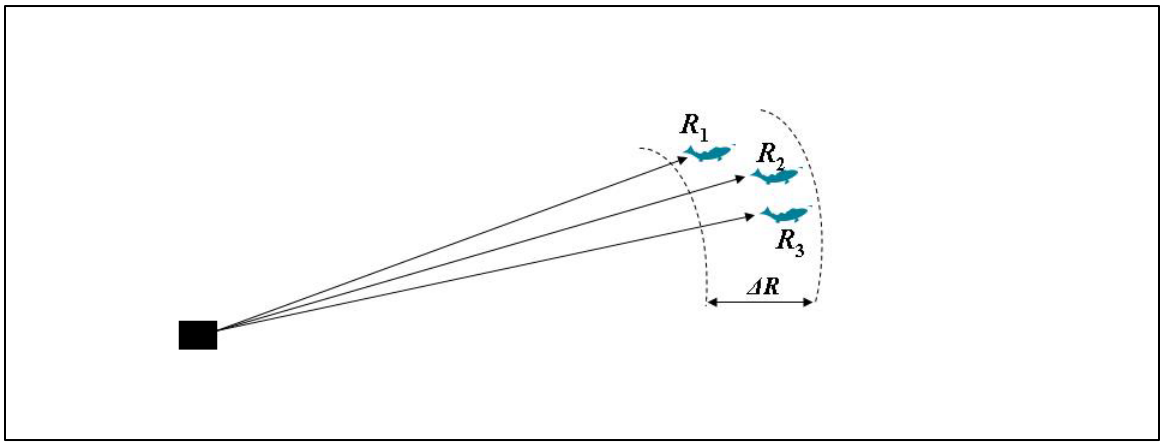

Figure A2. Geometry of the many-fish backscattering model where 3 fish are confined in a range shell with a thickness of ΔR which is much smaller than the ranges between the fish and the transducer.

According to (A7), the total echo from the 3 fish can be expressed as:

$$(A8) \quad p_e(t) = p_1 + p_2 + p_3 = \frac{D^2(\theta_1,\phi_1)\cdot A_0 \cdot \sqrt{\sigma_{bs1}}}{{R_1}^2}\cdot e^{-i2\pi f(t-2R_1/c)} + \frac{D^2(\theta_2,\phi_2)\cdot A_0 \cdot \sqrt{\sigma_{bs2}}}{{R_2}^2}\cdot e^{-i2\pi f(t-2R_2/c)} + \frac{D^2(\theta_3,\phi_3)\cdot A_0 \cdot \sqrt{\sigma_{bs3}}}{{R_3}^2}\cdot e^{-i2\pi f(t-2R_3/c)}$$

where p_1, p_2 and p_3 are echoes from the 3 fish respectively.

Ensemble averaging of squared echoes over many pings

By multiplying the conjugate of p_e to both sides of (A8), we arrive at:

$$(A9) \quad |p_e|^2 = p_e \cdot p_e^* = |p_1|^2 + |p_2|^2 + |p_3|^2 + 2|p_1|\cdot|p_2|\cdot cos(\phi_{12}) + 2|p_1|\cdot|p_3|\cdot cos(\phi_{13}) + 2|p_2|\cdot|p_3|\cdot cos(\phi_{23})$$

where φ_{ij} is the phase difference between echo signals from Fish i and j, and can be expressed as: $\phi_{ij} = 2\pi f[2(R_i - R_j)/c]$ (in radians).

Assuming the sonar projects *M* pings of pulses to insonify the 3 fish, and *M* is adequately large for the performance of a stable ensemble average of $|p_e|^2$, from (A9) we obtain the ensemble average of echoes over the *M* pings, denoted as $<|p_e|^2>$,

$$(A10) \quad < |p_e|^2 >=< |p_1|^2 > +< |p_2|^2 > +< |p_3|^2 > + 2 < |p_1| \cdot |p_2| \cdot cos(\phi_{12}) > + 2 < |p_1| \cdot |p_3| \cdot cos(\phi_{13}) > +2 < |p_2| \cdot |p_3| \cdot cos(\phi_{23}) >.$$

Since the 3 fish are closely spaced relative to their ranges to the transducer, and φ_{ij} are randomly distributed over the *M* pings, all cross-product terms vanish upon the ensemble averaging or can be ignored in comparisons to the magnitudes of the in-phase terms. This leads to

$$(A11) \quad < |p_e|^2 >=< |p_1|^2 > +< |p_2|^2 > +< |p_3|^2 > \cong \frac{A_0^2 \cdot \sigma_{bs}}{R^4} \cdot (D_1^4 + D_2^4 + D_3^4),$$

where *R* is the mean range from the transducer to the 3 fish; σ_{bs} is the mean backscattering cross-section of these fish; D_1, D_2, and D_3 are the values of the directivity function of the transducer to the 3 respective fish targets.

If there are *N* individual fish distributed in the range shell, (A11) becomes

$$(A12) \quad < |p_e|^2 >= \sum_{i=1}^{N} < |p_i|^2 > = \frac{A_0^2 \cdot \sigma_{bs}}{R^4} \cdot \sum_{i=1}^{N} D_i^4$$

where D_i (i = 1, 2..., *N*) are transducer's directivities to the *N* fish targets. Equation (A12) links the echo amplitude to the fish abundance *N* inside the volume of the range shell ΔR. This mathematic expression states that squared echo amplitude $<|p_e|^2>$ is not uniquely linked to fish abundance *N* unless fish locations or distributions inside the sound-beam are known to allow for a proper removal of the beam pattern effect $\sum_{i=1}^{N} D_i^4$ from the received echo. In other words, a smaller number of fish (a small *N*) distributed near the centre of the sound-beam can produce a similar echo amplitude to that from a larger number of fish distributed off the beam centre. Therefore, the key step in accurately estimating *N* from $<|p_e|^2>$ via the model is to estimate fish distribution inside the range shell.

Integration form of $\sum_{i=1}^{N} D_i^4$ *or Integrated Beam Pattern (IBP)*

The summation of the 4th power of directivities to the *N* fish can be expressed as a volumetric integration if the distribution of the *N* fish can be quantified by a density function ρ_f inside the volume *V* bounded by the range shell ΔR such that

$$(A13) \quad \sum_{i=1}^{N} D_i^4 = \int_V \rho_f \cdot D^4 \cdot dv.$$

Since $dv = ds \cdot dr = (r^2 \cdot d\Omega) \cdot dr = r^2 \cdot dr \cdot d\Omega$ where $d\Omega$ is an elementary solid angle encompassing the elementary area *ds*, this leads (A13) to:

$$\text{(A14)} \quad \sum_{i=1}^{N} D_i^4 = \int_V \rho_f \cdot D^4(\theta,\phi) \cdot dv = \int_{R-\Delta R/2}^{R+\Delta R/2} r^2 dr \int_{4\pi} \rho_f \cdot D^4(\theta,\phi) \cdot d\Omega.$$

Since in many practical problems, we do not have direct measurements of ρ_f, it is difficult to accurately evaluate the integration. In the following, we only evaluate (A14) assuming fish are uniformly distributed inside the range shell. Under this assumption, ρ_f =*constant*, the integration in (A14) can be significantly simplified to

$$\text{(A15)} \quad \sum_{i=1}^{N} D_i^4 = \rho_f \int_{R-\Delta R/2}^{R+\Delta R/2} r^2 dr \int_{4\pi} D^4(\theta,\phi) \cdot d\Omega = \rho_f \cdot \frac{(R+\Delta R/2)^3 - (R-\Delta R/2)^3}{3} \cdot \psi_e$$

where $\psi_e = \int_{4\pi} D^4(\theta,\phi) \cdot d\Omega$ is the integrated 2-way beam pattern (IBP) of the transducer. The 2-way IBP can be numerically evaluated if the transducer's 3-dB beam-width is known. Assuming the transducer's beam-pattern is defined by two orthogonal full beam angles, denoted as θ_w and θ_h, respectively, according to Probert-Jones (1962), ψ_e can be approximated by the following expression:

$$\text{(A16)} \quad \psi_e = \int_{4\pi} D^4(\theta,\phi) \cdot d\Omega \cong \frac{\pi \cdot \theta_w \cdot \theta_h}{8 \cdot ln\, 2},$$

where θ_w and θ_h are in radians.

For the 2nd factor in (A15), since $\Delta R << R$, it can be approximated through Taylor's expansions as:

$$\frac{(R+\Delta R/2)^3-(R-\Delta R/2)^3}{3} = \frac{R^3}{3} \cdot \{[1 + 3 \cdot \Delta R/(2R)+\ldots] - [1 - 3 \cdot \Delta R/(2R)+\ldots]\} \cong R^2 \cdot \Delta R.$$

With the above approximation, (A15) becomes

$$\text{(A17)} \quad \sum_{i=1}^{N} D_i^4 = \rho_f \cdot (R^2 \cdot \Delta R) \cdot \psi_e$$

Substituting (A17) into (A12), we obtain

$$\text{(A18)} \quad < |p_e|^2 >= \rho_f \cdot \sigma_{bs} \cdot \Delta R \cdot \frac{A_0^2}{R^2} \cdot \psi_e$$

Dividing both sides of (A18) by acoustic impedance of the water, we can use echo intensity I_e to replace echo pressure. This leads to

$$\text{(A19)} \quad I_e = sv \cdot \Delta R \cdot \frac{I_0}{R^2} \cdot \psi_e$$

where $sv = \rho_f \cdot \sigma_{bs}$ is the volume backscattering coefficient of the fish school inside the volume V bounded by the range shell ΔR; I_0, sound intensity at the source, is related to source level SL as $SL = 10 \log I_0$. Equation (A19) is the core model for acoustic probing of fish schools with volumes

much greater than the volume of the range shell ΔR. It also provides a mathematic link between the echo intensity and the volume backscattering coefficient of the fish school. Since echo intensities can be measured by a calibrated echo sounder, (A19) allows for a remote measurement of sv.

Integration of echoes from a school of fish

Fish schools usually occupy volumes significantly greater than the range shell volume. We can stratify the echo intensity signal with range (from a large school) by the range shell of ΔR. For each of the stratified echo intensities to a single ping, model (A19) links the intensity to the volume backscattering coefficient sv of the fish within a stratum. Therefore, by integrating the stratified echo intensity signals over the spatial range scale of the school, say, bounded by a range bin from R_1 to R_2, we can solve for the mean sv for the entire fish school. That is,

$$\text{(A20)} \quad EI = \int_{T_1}^{T_2} I_e \cdot dt = \Delta R \cdot I_0 \cdot \psi_e \int_{T_1}^{T_2} \frac{sv}{R^2} \cdot dt$$

where $T_1 = 2R_1/c$ and $T_2 = 2R_2/c$ (note these are 2-way travel times); $\Delta R = c\tau/2$. Introducing the mean volume backscattering coefficient $\overline{sv}$ for the school, and a mean range $\bar{R}$ to the school, $\overline{sv}$ can be solved from (A20) as

$$\text{(A21)} \quad \overline{sv} = \frac{\bar{R}^2 \int_{T_1}^{T_2} I_e dt}{I_0 \psi_e \tau (R_2 - R_1)}$$

If a digital sounder system digitizes the analog echo voltage at a sampling interval of δt, then (A21) can be expressed in a digital form of

$$\text{(A22)} \quad \overline{sv} = \frac{\bar{R}^2 \delta t \sum_{i=1}^{m} I_e(i)}{I_0 \psi_e \tau (R_2 - R_1)}$$

where m is the number of digital samples of I_e for a single ping. With (A22), the average volume density of the fish school q_v can be calculated as

$$\text{(A23)} \quad q_v = \frac{\overline{sv}}{\sigma_b}$$

Reference

Probert-Jones, J. R., 1962. The radar equation in meteorology. Quarterly Journal of Royal Meteorological Society. Vol. 88, pp. 485-495.

FINANCIAL STATEMENT

Pacific Salmon Commission

A pilot study on the application of hydroacoustic surveys to assess the abundance of delaying sockeye in southern Georgia Strait

Statement of Receipts and Expenditures

As at: **November 30, 2019**

	ACTUAL	BUDGET	Variance
Receipts			
Project Grant	$ 43,875.00	$ 48,772.50	$ 4,897.50
Total receipts	$ 43,875.00	$ 48,772.50	$ 4,897.50
Expenditures			
Labour Costs	$ 29,096.99	$ 41,850.00	$ 12,753.01
Site/ Project Costs	$ 11,368.30	$ 3,000.00	$ (8,368.30)
Administration	$ 2,322.50	$ 2,322.50	$ -
Capital Costs	$ 1,643.29	$ 1,600.00	$ (43.29)
Total Expenditures	$ 44,431.08	$ 48,772.50	$ 4,341.42
Balance	$ (556.08)	$ -	$ 556.08

I certify the information given above is, to the best of my knowledge, correct and complete

Date: January 9, 2020 Signature:

Witty Lam

Position: Senior Accountant